X 90-36156

X90-36156 *

NASA Contractor Report 4335

Available to NASA Personnel only

Strength Scaling in Fiber Composites

Sotiris Kellas and John Morton

CONTRACT NAS1-18471
NOVEMBER 1990

NASA

NASA Contractor Report 4335

Strength Scaling in Fiber Composites

Sotiris Kellas and John Morton
Virginia Polytechnic Institute and State University
Blacksburg, Virginia

Prepared for
Langley Research Center
under Contract NAS1-18471

NASA
National Aeronautics and
Space Administration
Office of Management
Scientific and Technical
Information Division

1990

STRENGTH SCALING IN FIBER COMPOSITES

Sotiris Kellas

and

John Morton

Department of Engineering Science and Mechanics
Virginia Polytechnic Institute and State University
Blacksburg, VA 24061-0219

ABSTRACT

A research program has been initiated to study and isolate the factors responsible for scale effects in the tensile strength of graphite/epoxy composite laminates.

Four lay-ups, $(\pm 30°_n/90°_{2n})_s$, $(\pm 45°_n/0°_n/90°_n)_s$, $(90°_n/0°_n/90°_n/0°_n)_s$, and $(\pm 45°_n/\pm 45°_n)_s$, have been chosen with appropriate stacking sequences so as to highlight individual and interacting failure modes. Four scale sizes have been selected for investigation including full scale size, 3/4, 2/4, and 1/4, with n equal to 4, 3, 2, and 1, respectively. The full scale specimen size was 32 plies thick as compared to 24, 16, and 8 plies for the 3/4, 2/4, and 1/4 specimen sizes respectively.

Results were obtained in the form of tensile strength, Stress/strain curves and damage development. Problems associated with strength degradation with increasing specimen size have been isolated and discussed. Inconsistencies associated with strain measurements have also been identified. Enhanced X-ray radiography was employed for damage evaluation, following step loading.

It has been shown that fiber dominated lay-ups were less sensitive to scaling effects compared to the matrix dominated lay-ups. Further, it has been shown that fabrication induced damage was partly responsible for the observed behavior.

Extrapolation to the full scale strength was attempted by means of three basic methods: a Weibull statistics based model, a fracture mechanics based model, and a combination model involving the previous two models in conjunction with a failure criterion. The predictive performance of each one of these models has been assessed and their applicability to the present problem has been discussed.

ACKNOWLEDGEMENTS

This study was supported by NASA Langley research center under NASA Grant NAS1-18471. Thanks are due to the contract monitor Huey D. Carden. The help of Karen E. Jackson is gratefully acknowledged also.

LIST OF TABLES

Table 1. Specimen geometric details.

Table 2. Summary of the Experimental strength and failure strain results.

Table 3. Summary of the longitudinal initial stiffness.

Table 4. Comparison of measured and calculated tensile strengths.

Table 5. Material properties used for strength and stiffness prediction. Values supplied by material manufacturer.

Table 6. Material properties used for strength and stiffness prediction. Values were reported in [11].

Table 7. Material properties used for the full scale strength prediction. Calculations for Strength were based on initial values according to Table 5.

Table 8. Strength predictions for the full scale specimens.

LIST OF FIGURES

Figure 1. Custom built extensometers.

Figure 2. Strain gage instrumented specimens.

Figure 3. Stress/strain response for lay-up **A**.

Figure 4. Stress/strain response for lay-up **B**.

Figure 5. Stress/strain response for lay-up **C**.

Figure 6. Stress/strain response for lay-up **D**.

Figure 7. Typical modes of final failure of lay-up **A**.

Figure 8. Typical modes of final failure of lay-up **B**.

Figure 9. Typical modes of final failure of lay-up **C**.

Figure 10. Typical modes of final failure of lay-up **D**.

Figure 11. Typical edge replicas in three different lay-ups (**A**, **B** and **C**).

Figure 12. X-ray radiographs of virgin specimens of lay-up **A**.

Figure 13. X-ray radiographs of virgin specimens of lay-up **B**.

Figure 14. X-ray radiographs of virgin specimens of lay-up **D**.

Figure 15. X-ray radiographs of pre-loaded specimens of lay-up **A**. Applied stress equal to 15 ksi.

Figure 16. X-ray radiographs of pre-loaded specimens of lay-up **B**. Applied stress equal to 30 ksi.

Figure 17. X-ray radiographs of pre-loaded specimens of lay-up **B**. Applied stress equal to 45 ksi.

Figure 18. X-ray radiographs of pre-loaded specimens of lay-up **C**. Applied stress equal to 69 ksi.

Figure 19. X-ray radiographs of pre-loaded specimens of lay-up **D**. Applied stress equal to 12 ksi.

Figure 20. X-ray radiographs of pre-loaded specimens of size 1/4,and 2/4 for all four lay-ups. All specimens were loaded to near failure.

Figure 21. Crack density versus applied stress in individual groups of plies in lay-up **A**.

Figure 22. Crack density versus applied stress in individual groups of plies in lay-up **B**.

Figure 23. Crack density versus applied stress in individual groups of plies in lay-up **C**.

Figure 24. Crack density versus applied stress in individual groups of plies in lay-up **D**.

Figure 25. Free edge x-displacement distribution, for lay-up **B**, by moire' interferometry.

Figure 26. Free edge z-displacement distribution, for lay-up **B**, by moire' interferometry.

Figure 27. Residual stress in the 90° plies of a $(0°_m/90°_n)_s$ laminate versus the m/n ratio.

Figure 28. Strength versus ply thickness for the 90° plies of lay-up **B**, $(\pm 45°_n/0°_n/90°_n)_s$, based on strength predictions by Eqs. 2 and 3.

Figure 29. Delamination stress versus n for a quasi-isotropic lay-up $(\pm 45°_n/0°_n/90°_n)_s$. A comparison between theory by [7], experiment by [7], and Eq.3 by [8].

Figure 30. Correlation between the fracture mechanics based model, Eq.3, and the experimentally obtained strengths for lay-ups **A**, **B**, **C**, and **D**.

Figure 31. A comparison of the predictive performance between the fracture mechanics based model, Eq.3 and the Weibull statistics based model Eq.2.

Figure 32. Calculated strength versus the matrix degradation factor, [9], for lay-ups **A**, **B**, **C**, and **D**. The strength calculation was based upon the quadratic failure criterion with the strength interaction F^*_{12} assumed to be equal to -0.5.

Figure 33. Normalized strength versus specimen size for lay-ups **A**, **B**, **C**, and **D**. A summary of the experimental results.

Figure 34. Normalized strain to failure versus specimen size for lay-ups **A**, **B**, **C**, and **D**. A summary of the experimental results.

INDEX

1. INTRODUCTION **7**

2. EXPERIMENTAL PROCEDURE **10**
2.1 Lay-ups 10
2.2 Specimen Geometry 10
2.3 Mechanical Testing 11
2.4 Damage Evaluation 11
2.5 Edge Stress Evaluation 12
Photomechanics
Finite Element Analysis
2.6 Apparatus 13
Loading Frame
Extensometers
Data Acquisition

3. RESULTS **15**
3.1 Tensile Strength 15
3.2 Tensile Stiffness 15
3.3 Failure Modes 16
Lay-Up A
Lay-Up B
Lay-Up C
Lay-Up D
3.4 Non Destructive Examination 18
3.5 Edge Stress Evaluation 19
Photomechanics

4. DISCUSSION **21**
4.1 Experimental Program 21
4.2 Damage 21
4.3 Strength 26
4.4 Failure Strain 34
4.5 Stiffness 35

5. CONCLUSIONS **38**
5.1 Damage 38
5.2 Strength 38
5.3 Failure Strain 39
5.4 Stiffness 40

6. SUGGESTED FURTHER WORK **41**

REFERENCES **42**

TABLES **43**

FIGURES **47**

1. INTRODUCTION

Many engineering structures evolve from small scale models, which can be manufactured and tested under controlled laboratory conditions. Consequently, it is important that any effects associated with scaling be identified, well understood, and correlated to model size. Also, in the case of advanced composites, material properties such as strength and stiffness are obtained from small coupons tested under laboratory conditions. It is important to determine whether such measurements are representative of the behavior of large scale components.

Due to the intricacy of their internal microstructure, fiber reinforced composite materials belong to a special category of materials presenting some complex and hence challenging scaling problems. Complications may arise from factors upon which standard similitude laws cannot be satisfied. Such factors are; fabrication, fiber diameter, fiber/matrix interface, ply interface, and test method. If these limitations are disregarded, one is then left with two obvious scaling options for laminated composite materials: (a) ply-level scaling which, superficially, appears to be the best one of the two options, and (b) sublaminate-level scaling. Ply-level scaling is achieved when a large scale laminate, of a given stacking sequence, is constructed from thick layers of the same fiber orientation, each built from a number of standard thickness plies. On the other hand, sublaminate-level scaling is achieved by the introduction of basic sublaminates which are stacked together to form thicker laminates. For example, $(+45°/-45°/0°)_s$ and $(+45°_4/-45°_4/0°_4)_s$ are said to be scaled at a ply level, whereas $(+45°/-45°/0°)_s$ and $(+45°/-45°/0°)_{4s}$ are said to be scaled at a sublaminate level where, (+45°/-45°/0°) is the sublaminate.

Previous research, [1-7], has shown that the strength and stiffness of fiber reinforced composite materials depend upon the size of the composite laminates. It has been demonstrated that the degree of influence depends upon the type of scaling level used, the stacking sequence, and the mode of loading. For example, Lagace *et al* [4], presented results which showed that each of the three ply-level scaled laminates; $(\pm 15_n)_s$, $(\pm 15_n/0_n)_s$ and $(0_n/\pm 15_n)_s$ exhibited a different tensile strength degradation when n was increased from 1 to 5. The same authors have shown that the tensile strength of otherwise similar, sublaminate-level scaled, laminates remained unchanged when n was varied from 1 to 3. In conclusion, these authors have attributed the problem of strength degradation to interlaminar stress effects. Similar conclusions were reported by Rodini and Eisenmann [7].

Camponeschi [5], on the other hand, has presented compression data, which indicate strength degradation in sublaminate level scaled laminates. Furthermore, he showed that the degree of compressive strength degradation depends upon the material system as well as the laminate thickness.

As a result of the complexity of the problem due to the large number of variables involved (geometry, material system, lay-up, stacking sequence, environment, and loading mode), research studies, to-date, have failed to establish the exact causes of strength degradation in scaled composite laminates. Consequently, various researchers have different views on what is causing the scale effect. Some have associated the problem with edge effects, [4], while others have attacked the problem from a statistical point of view, [1 and 6], or a combination of the two, [7]. Some have considered the fracture mechanics approach, [8]. Batdorf [6], for example, has proposed a size relationship for plain (unnotched) unidirectional composites which is a slightly modified version of the Weibull theory which states that the size-strength relationship of **brittle materials** failing in tension is given by:

$$\ln S(V) = C - \left(\frac{1}{m}\right) \ln V \tag{1}$$

where S is the material tensile strength, V is the volume of the material under stress, C is a constant, and m is a shape parameter. For geometrically similar **brittle materials**, Eq.1 may be written as:

$$\frac{S_1^{ult}}{S_2^{ult}} = \left(\frac{V_2}{V_1}\right)^{\frac{1}{m}} \tag{2}$$

where the shape parameter m is a constant for a given material. Thus, if m can be evaluated from two small size specimens, the strength of geometrically similar large size components can be predicted.

Atkins and Caddell [8] used a fracture mechanics approach to derive a simple size-strength relationship for notched brittle materials. Using elementary similitude laws they have shown that the stress, σ_f, required to propagate a crack in a full scale structure and the corresponding stress, σ_m, in a model structure are related by:

$$\sigma_f = \frac{\sigma_m}{\sqrt{\lambda}} \tag{3}$$

where λ is a geometric scaling factor (ratio of full scale to model dimension).

The objective of the present work is to study and isolate the factors responsible for scale effects on the tensile strength of graphite reinforced epoxy laminates. A single graphite reinforced epoxy system has been studied, Magnamite AS4/3502. Four different lay-ups and four specimen sizes were selected; from full scale down to quarter scale. All laminates were scaled at the "ply level". Standard geometric similitude laws were followed in scaling specimens in all three dimensions, gage length, width, and thickness. The four lay-ups are; $(\pm 30°_n/90°_{2n})_s$, $(\pm 45°_n/0°_n/90°_n)_s$, $(90°_n/0°_n/90°_n/0°_n)_s$, and $(\pm 45°_n/\pm 45°_n)_s$. These laminate stacking sequences were chosen so as to highlight individual and interacting failure modes. The strain in loaded specimens was recorded in two different ways: (a) with the aid of "scaled" custom-built extensometers and (b) with strain gages. Enhanced X-ray radiography was used extensively in the assessment of damage in pre-loaded specimens.

The statistical and fracture mechanics models, given in Eqs. 2 and 3 respectively, and a quadratic failure criterion [9] used in conjunction with Eqs. 2 and 3, were employed in a comparison of predicted and measured strengths. The usefulness and limitations of these empirical models and criteria are discussed. Recommendations are made concerning applications of these models for the prediction of the strength of large laminates based on experimental data derived from small specimens.

2. *EXPERIMENTAL PROCEDURE*

Four lay-ups and four scale sizes have been selected for investigation; full scale size, 3/4, 2/4, and 1/4. The full scale specimen size was 32 plies thick as compared to 24, 16, and 8 plies for the 3/4, 2/4, and 1/4 specimen sizes respectively. At least one of the four specimen sizes complied with the ASTM D 3039 standard specimen geometry for the determination of the tensile properties of fiber-resin composites. This was chosen so that results could also be interpreted in terms of departure from "standard properties".

2.1 Lay-ups

The stacking sequence for each one of the four lay-ups is summarized below:

(a) $(+30°_n/-30°_n/90°_{2n})_S$ denoted **A**;

(b) $(+45°_n/-45°_n/0°_n/90°_n)_S$ denoted **B**;

(c) $(90°_n/0°_n/90°_n/0°_n)_S$ denoted **C** and,

(d) $(+45°_n/-45°_n/+45°_n/-45°_n)_S$ denoted **D**, where, n=1,2,3 or 4 corresponding to 1/4, 2/4, 3/4, and full scale respectively.

Note that none of the four families of lay-ups have 0° plies on the surface. These were selected so as to minimize the need for specimen end tabs. Instead, abrasive cloth was used between the jaws and the specimen for improved gripping.

2.2 Specimen Geometry

Following fabrication all panels were stored in a controlled dry environment. Prior to specimen preparation all panels were C-scanned for quality evaluation. Coupon specimens were cut from the panels using a high precision diamond saw. This ensured both parallel as well as flat and smooth specimen free edges. During cutting, panels were clamped firmly along the total cutting length to reduce or eliminate edge damage due to vibration. For the same reason, the linear speed of the cutting wheel was appropriately adjusted for the different panel thicknesses (the larger the thickness the lower the linear speed). All specimens were stored in a nominally dry environment (room

temperature, 0% RH) thus ensuring a uniform environmental exposure during testing. Specimen geometric details as well as the number of available specimens per size are shown in table 1.

The experimental program was divided into two parts:

(a) a preliminary program in which the usefulness of several damage examination techniques was assessed. Approximate values for strength and failure strain were also established and,

(b) a main program in which specimens were tested following given guidelines, set according to the preliminary findings.

2.3 Mechanical Testing

In the preliminary part of the program minimal specimen instrumentation was used. Load versus cross head displacement were read directly from the testing machine into an IBM PC. In the main part of the program, careful monitoring of the Stress/strain behavior was achieved through the use of a more advanced data acquisition system and specimen instrumentation. For approximately eight specimens per lay-up and size, strain was monitored using custom built extensometers, as shown in figure 1. Four extensometers were designed and fabricated to accommodate the four scaled specimen sizes. The observed stress/strain behavior was then verified against specimens instrumented with both strain gages and extensometers. Only one specimen per lay-up and size was tested in this way. Specimens with lay-ups **A**, **B** and **D** were instrumented with both a series of central gages as well as one "edge" gage. However, specimens of lay-up **C** were instrumented with a single central gage. The manner in which specimens were instrumented with gages is shown in figure 2.

2.4 Damage Evaluation

Penetrant enhanced X-ray radiography was employed as a non-destructive damage evaluation technique. Specimens were soaked in zinc-iodide solution prior to being X-rayed in a Faxitron Series 43805N X-ray cabinet. Damage was recorded on M5 Kodak X-ray film. Since the same specimen

was used in a load increment/damage evaluation procedure, it was assumed that the penetrant solution had no effect upon the fracture characteristics of the epoxy. To validate this assumption, tests for a given specimen were carried out in as short a period as possible to reduce the amount of penetrant absorbed by the matrix.

At least one virgin specimen per lay-up and scale size was radiographed for an initial quality assessment. These specimens were further evaluated by X-ray radiography after proof loading in which specimens were loaded to a predetermined percentage of thier respective failure loads and then unloaded. Several sequential loading increments per specimen were used, each one followed by damage evaluation using X-ray radiography. The load increments were determined from the predetermined Stress/strain plots.

Edge replication was also used to assess edge damage propagation following a proof load. However, compared to X-ray radiography, edge replication did not offer additional useful information. Therefore, the use of edge replication was limited to preliminary tests.

The specimen fracture surfaces were also examined and the modes of failure were documented. Typical fractured specimens were selected and photographed.

2.5 Edge Stress Evaluation

Photomechanics

The edge stress (strain) distribution, for all four lay-up configurations, was studied by photomechanics. High sensitivity moire' gratings were replicated at the edges of specimens (3/4 and 4/4 sizes only). Displacement fields in two mutually perpendicular directions, loading and thickness which are denoted u and v respectively, were obtained at various applied loads.

Finite Element Analysis

Edge stresses were studied analytically using three dimensional finite element models. Two models were designed. In the first one individual blocks of identical plies were modeled as one orthotropic linear elastic region. In the second model additional thin isotropic regions, representing the resin rich ply-interface were inserted between the orthotropic regions. Due to region thickness constraints, refined meshes contained a very large number of elements. Even so, based on the accuracy of the results, the finite element model proved to be inadequate in predicting the true stress distribution at the free edges. Furthermore, available software at the time were incapable of non-linear elastic analysis which was thought to be the most appropriate analysis for this kind of application. Therefore, the finite analysis method was terminated.

2.6 Apparatus

Loading Frame

All tests were performed at a constant rate of displacement on a 120 kip capacity "Tinius Olsen" screw driven test machine, equipped with mechanical wedge type grips. In the case of the two small specimen sizes a pair of 20 kip "Instron" grips were adapted and used. The replacement of the "Tinius Olsen" original grips was necessary due to space constraints between the machine's cross heads. The two larger specimen sizes were tested in the original grips. Due to the dependance of strength on specimen size it was concluded that performing all tests on the same machine was a more important condition than the change of the grips, provided that only valid failures would be considered. Valid failures were defined as those occurring within the specimen gage length. Test results from specimens with grip induced failures were rejected unless their measured strength happened to be higher than the average strength obtained from valid tests.

The rate of cross-head displacement was 0.1, 0.2, 0.3, and 0.4 in./minute for sizes 1/4, 2/4, 3/4, and full scale size respectively; that is, specimens were tested at approximately the same strain rate.

Extensometers

Four scaled extensometers, figure 1, were designed, built, and tested according to the specific requirements of the experimental program. Both the effective gage length and the knife-edge width were scaled. The extensometers were mounted on the specimens with the aid of elastic bands. The minimum pressure, provided by the bands to ensure "no-slip", was determined from a series of preliminary tests on aluminum specimens.

The extensometers were calibrated in two ways: (a) using a displacement calibrator, in which case the bridge output was recorded after a given applied extension, and (b) using an aluminum specimen instrumented with strain gages. Good agreement between the two calibration methods was obtained. Thus, it was established that all four extensometers were capable of a repeatable linear response within the designed strain range, 0-2% strain.

Data Acquisition

Data were acquired in an Apple Macintosh model SE equipped with a data acquisition system (hardware and software) supplied by Strawberry Tree Inc. Both the load and strain gage readings from a strain gage amplifier were stored directly on the hard disk. The cross head displacement was not monitored.

3. *RESULTS*

3.1 Tensile Strength

A summary of the tensile strength results is provided in table 2. Both the failure stress and strain values as well as the normalized values of stress and strain-to-failure are indicated. Strength is defined as the maximum attained load divided by the measured cross sectional area of each specimen. Likewise, failure strain is defined as the maximum recorded displacement divided by the the extensometer gage length. There are at least three points worth noting in table 2:

(1) The tensile strength depends upon the specimen size: the greater the size the smaller the strength. This is true for all four lay-ups. However, the degree of influence depends upon the percentage of 0° plies in a given lay-up; the more 0° plies the lower the strength related scaling effect.

(2) So far as the strength is concerned the scaling effect appears to be diminished with increasing specimen size; that is, it would appear that when a certain specimen size is reached (not necessarily the full scale size used here), scaling effects tend to a limiting value.

(3) The failure strain is also affected by the specimen size. However, it appears that the failure strain depends upon the stacking sequence rather than just the number of 0° plies in a given laminate.

3.2 Tensile Stiffness

The stiffness for each specimen type was determined from the Stress/strain curves, obtained from both the extensometer and the strain gage readout. Apart from lay-up **C**, specimens from all other lay-ups exhibited a non-linear Stress/strain response, as shown in figures 3, 4, 5 and 6 for lay-ups **A**, **B**, **C** and **D** respectively. Therefore, the reported values for stiffness, shown in table 3, represent the initial slope of these curves, and are valid for small strains only. At this point it should be noted that the Stress/strain curves which are shown in figures 3-6, were obtained from a single test on a representative specimen of each size and lay-up. The Stress/strain data were collected simultaneously from the individual strain gages and the extensometer.

Even though the stiffness value derived from strain-gage data is not strictly statistically meaningful, the results listed in table 3 suggest that, for small strains at least, the value of the measured stiffness is independent of the method and location of measurement. Furthermore, it would appear from the results that all specimen sizes, of a particular lay-up, share approximately the same initial stiffness value. However, the total Stress/strain response appears to depend upon the lay-up, the specimen size, and the method of measurement. For example, specimens of lay-up **C** displayed approximately the same Stress/strain response throughout the loading range, as shown in figure 5. (Note, small discontinuities in these plots represent extensometer jumping associated with energy release during the occurrence of damage). On the other hand, specimens of lay-up **B**, shown in figure 4, exhibited a Stress/strain response which was more sensitive to specimen size and the method of strain measurement. It was observed that a sudden drop in stiffness in the full scale specimen which was detected by the extensometer was not registered by the strain gages. This sudden drop in stiffness was later found to be associated with the formation of delamination. Furthermore, it was observed that strain gages were inadequate in providing a true measure of the failure strain, since gages were usually damaged (detached) prior to specimen final failure. Another difference between the extensometer and the strain gage reading is depicted in figures 3 and 6, where the extensometer reading suggests a slight increase in specimen stiffness with increasing size and applied load.

3.3 Failure Modes

Final modes of failure are shown in figures 7-10 for lay-ups **A-D** respectively. It is of interest to note that for the fiber dominated lay-ups (**B** and **C**) the modes of failure depended upon the specimen size. In fact, contrary to the strength behavior, the lay-up containing the largest amounts of 0° plies was much more sensitive to failure mode related scaling effects than laminates with less or no 0° plies. For example, so far as the tensile strength is concerned, specimens of lay-up **C** (50% 0° plies) showed very little dependance upon size. However, even though the strength in all four sizes was comparable, the mode of failure was completely different, as depicted in figure 9. The mode of failure changed from a clean fracture in the 1/4 size specimens to a brush-like fracture in the full scale

specimens. On the other hand, specimens of lay-up **A** and **D** (no 0° plies) which showed large strength related size dependency, exhibited no apparent failure related size effects, as indicated in figures 7 and 10.

Lay-Up A $(+30°_n/-30°_n/90°_{2n})_S$

One major difference in the observed fracture modes between the different size specimens is that, in general, small size specimens appeared to have suffered somewhat more delamination between the -30° and 90° plies at failure. Apart from the delamination size between the -30°/90° plies the overall mode of final failure was very similar in all four sizes , as shown in figure 7.

Lay-Up B $(+45°_n/-45°_n/0°_n/90°_n)_S$

In this case the mode of final failure underwent a transition with increasing specimen size, from a localized type of fracture in the small specimens to an extensive fracture in the large specimens, as shown in figure 8. Furthermore, small specimens exhibited delamination in the 0°/90° interface as opposed to "delamination" between all interfaces in the larger sizes.

Lay-Up C $(90°_n/0°_n/90°_n/0°_n)_S$

This family of specimens displayed the most pronounced transition in their mode of final failure which changed from a clean and localized fracture in the small specimens to an extensive fracture occupying the whole gage length in the large specimens , as shown in figure 9.

Lay-Up D $(+45°_n/-45°_n/+45°_n/-45°_n)_S$

All four specimen sizes shared a very similar final failure mode (figure 10) which was a localized ±45° (shear) fracture with minor delamination between the ±45° interfaces.

3.4 Non Destructive Examination

Following curing and post curing, all panels were C-scanned for quality evaluation. Results indicated a slight but consistent deterioration in panel quality with panel thickness. This was particularly true in an area close to the panel edges.

Edge Replication

Sample edge replicas were taken during preliminary investigations. Examples are shown for 1/4 size specimens in figure 11 for three lay-ups (**A**, **B** and **C**) at two different load cases. The technique, although simple in its application, is inadequate in providing fine detail, which could be achieved by enhanced X-ray radiography.

X-ray Radiography

X-ray radiography was used extensively in the assessment of damage following incremental load application. Figures 12-14 indicate that even before load is applied, large size specimens contain substantial interply matrix damage. From these results it would appear that matrix damage is related to lay-up configurations but also depends upon the number of plies grouped in a given lay-up. It is believed that at least some of the observed cracks, in virgin specimens, has been triggered by specimen cutting, or simply by the generation of free edge stresses. However, the driving mechanism is not well understood.

The evolution of damage (transverse cracks and delamination) with increasing applied load was further monitored by enhanced X-ray radiography and documented in figures 15-20. The crack density (number of cracks per inch) as a function of the applied load is presented in figures 21-24, for lay-ups **A**-**D** respectively. Data points in these plots represent average values measured over the whole specimen gage length. For this evaluation, data from only one specimen per lay-up and size were available. It is interesting to note, as a general conclusion, that the crack density is a function of the applied load. Furthermore, fiber splitting appears to be dependent upon the ply constraints (lay-up) as well as ply thickness for a given lay-up.

In most cases, delamination appeared to have evolved as a result of extensive matrix damage at the specimen's free edges. Such delamination was more pronounced and, in general, appeared at a lower percentage of strength in the large size specimens. For example, for lay-up A, figure 15 shows that delamination has occurred in the full scale size specimen at 15ksi (approximately 90% of the average value of strength). On the other hand, figure 20 shows that delamination in the 2/4 scale specimens has occurred at 22ksi (approximately 97% of the average value of strength). Likewise, figures 16 and 20 show that delamination, along the entire gage length, is evident in the full and 1/4 scale size quasi-isotropic specimens, respectively, when the applied stress was 30 and 60 ksi. These stresses coresponded to 51% of the average failure stress for the full scale size specimen as compared to 74% of the failure stress for the 1/4 scale size specimen. Clearly, this is an indication of the interaction between transverse cracks and delamination. When transverse cracks reach a critical density, delamination initiates. Furthermore, it will be shown, in the discussion section that such behavior is responsible for the observed size effects on the modes of final failure.

3.5 Edge Stress Evaluation

Photomechanics

Typical examples of free-edge displacement fields, obtained by moire' interferometry, for the quasi-isotropic lay-up are shown in figures 25 and 26; for u (longitudinal) and v (through the thickness) displacements, respectively. Even though moire' is the most appropriate technique for this kind of application, the results from the present study are not as useful as one would expect. The epoxy which was used to transfer the grading on the edges of the specimens, had filled-in the pre-existing cracks which reappeared after initial loading. Therefore, a clear distinction between old and new cracks, at low applied loads, could not be made. However, the strain redistribution after the formation of an edge crack is obvious, with normal strains in the "uncracked plies" being replaced by large shear strains once a crack is fully formed within the whole ply thickness. Such large shear strains must be responsible for the observed delamination, shown in figure 25, for values of increased applied stress, for lay-up **B**. Additional useful information is the indication of applied load

induced cracking in the ±45° plies. As the applied load increases (to 17.5ksi for the quasi-isotropic specimens) such cracks appeared to have initiated in the surface plies first, as indicated in figure 25.

4. DISCUSSION

4.1 Experimental Program

Laminate stacking sequences were chosen so as to promote a variety of failure mechanisms including fiber fracture, delamination, and matrix transverse cracking. By doing so, at least one structurally inadequate lay-up had to be considered, lay-up **A**. The specimen minimum and maximum sizes were selected to satisfy certain constraints. The first constraint was set by test standards. For example, the 2/4 scale specimen size was chosen to comply with existing ASTM standards for specimen geometry. The second constraint was set by the capacity of the loading frame. This determined the limit for the "full scale" specimen size. Every possible effort was expended to ensure uniform curing and postcuring, uniform specimen cutting, ply-level scaling (as opposed to sublaminate scaling), and controlled (specimen) environmental exposure. However, unforeseen problems did arise, such as fabrication-induced matrix cracks in the grouped plies, which proved to be one the most important strength and stiffness controlling factors in the present study.

4.2 Damage

Interply cracks, which are often referred to as transverse matrix cracks, were formed during cutting and propagated transversely, along the fiber direction, from one free edge to the other. Such cracks were more dense in specimens with thick plies. Some cracks may have pre-existed in the uncut panels, however since the ultrasonic C-scanning technique is not sensitive enough to distinguish between a collection of microvoids and a collection of matrix microcracks, the pre-existence of the cracks could not be verified. Thus, it is assumed that cutting or large free edge stresses, or a combination of the two, are responsible for triggering these cracks. In addition to the triggering mechanism there must have existed a driving mechanism that would cause the cracks to propagate. It is generally accepted that thick laminates, scaled on a ply-level, may suffer more from free edge stresses compared to corresponding thin laminates [4 and 7]. Such stresses, however, cannot be solely responsible for the observed cracks, since delamination rather than transverse cracking would be a more appropriate resulting damage mode.

Residual curing stresses could also be responsible for driving the cracks since these stresses possess all the right attributes (sign and direction) to give rise to the observed damage. However, lamination theory would suggest that residual stresses should be the same in all scaled sizes for a given lay-up. Thus, if matrix cracks should develop due to curing stresses, these should be observed in all four sizes, and not only in the laminates with the thickest plies. A reasonable question then arises; is lamination theory applicable to the present problem? How good are the plane stress assumptions which are employed in the derivation of the theory? Work by several authors, such as: [7, 8 and 10] suggests that the stress required to form a crack depends upon the specimen size (or ply thickness in the present case).

Atkins and Caddell [8] used fracture mechanics in conjunction with simple similitude laws to derive a relationship, Eq.3, between the stress, σ_f, required to propagate a crack in a full scale structure and the corresponding stress, σ_m, in a model structure. If Eq.3 is applied to scaled, cross plied laminates, and assuming that preexisting microcracks, or voids, in the material will propagate as a result of the residual stress in the 90° plies, then, $(0°_n/90°_n)_s$ scaled laminates with large ns will crack at a lower stress. In addition, the strength of the 90° plies in a $(0°_m/90°_n)_s$ laminate must be a function of the relative thickness of the 0° and 90° plies, since the residual stress in the 90° plies depends upon the ratio m/n as shown in figure 27. Therefore, as n and/or the ratio m/n increases, the strength of the 90° plies will decrease.

Likewise, Weibull's statistical approach for brittle materials states that, a larger specimen is expected to have a higher concentration of voids and imperfections and, therefore, a lower strength than an identical but smaller sample of material. Hence, the strength of geometrically similar models, made from the same material, should decrease with increasing size according to Eq.2. Provided that the stress in the 90° plies required to initiate damage is known in at least two scaled specimens, the shape parameter m can be evaluated. Applying Eq.2 to the 90° plies of lay up B, $(\pm45°_n/0°_n/90°_n)_s$, an estimate for m of 8.8 is obtained. This value was calculated using approximate stress values for

transverse crack initiation in 1/4 and 3/4 scale sizes. Note that at an applied stress of 30 ksi the 90°-ply crack density in the 1/4 scale size was 1.3 cracks/inch and at zero applied stress the 90°-ply crack density in the 3/4 scale size was 2.7 cracks/inch. Thus, the actual stress carried by the 90° plies was calculated from lamination theory using an applied stress of 28 ksi and 0 ksi for the 1/4 and 3/4 scale sizes respectively. In both cases the temperature difference, responsible for the residual stresses, was assumed to be -180 °F. This produces a residual stress in the 90° plies equal to 4.42 ksi. Since the transverse cracks in the 3/4 scale size were already developed at zero applied load, a value of crack initiation stress of 4 ksi, which is slightly lower than the 4.42 ksi residual stress value, was chosen.

Using the 3/4 size specimen as the model it can be shown that both the fracture mechanics and Weibull based models predict a similar behavior, as shown in figure 28. Since the strength of the 90° plies is reduced with increasing ply thickness, first ply failure, as predicted by either Eqs. 2 or 3, will occur when the stress carried by the 90° plies reaches the failure stress. In the case of the 3/4 size specimen the stress in the 90° plies was purely a result of the residual stress, whereas in the case of the 1/4 size specimen the failure stress in the 90° plies, of the quasi-isotropic lay-up B, was reached by the combined effect of the residual and the applied stress. Note that the residual stress, for a given 90° ply thickness, can approach the limiting strength value also if the ply constraint is changed as indicated in figure 27. Clearly, with more available data, similar empirical plots, to that of figure 28, could have been obtained for the other three lay-ups. More generally, an estimate of the expected residual stress in the 90° plies for a given lay-up, together with an empirical plot such as those in figure 28, could be used in the prediction of the maximum ply thickness that can be used before cracking can occur in virgin ply level scaled laminates. In the case of Eq.3 experimental data (first ply failure stress) from only one specimen is needed, while in the case of Eq.2, at least, two experimental data points are necessary.

The influence of the 90° ply thickness in cross plied laminates has been studied amongst others by Wang [10]. He has shown that the applied stress (or applied strain) required to produce transverse

cracks, in cross plied laminates, depends upon the absolute thickness of the 90° plies. The thicker the 90° plies the lower the first ply failure is. This was supported both by analytical as well as experimental results.

It is perhaps worth noting that, with the exception of one previously reported case of cracked specimens of the same material system [11], there have been no other reports of cracked virgin laminates. For example, Highsmith and Reifsnider [12] studied the relationship of transverse cracks and applied load for $(0°/90°_3)_s$ E-glass epoxy specimens. Likewise, Wang [10] has reported results from a similar study for T300/934 and AS-3501-06 graphite epoxy systems with stacking sequences $(0°/90°_2)_s$ and $(0°_2/90°_3)_s$ respectively. In neither study were cracks reported in virgin specimens. The reason for the absence of cracks in their virgin specimens, as compared to the specimens used in the present research, may be attributed to a low m/n ratio. For example, if n>m the m/n ratio for a $(0°_m/90°_n)_s$ laminate is lower than that for a $(0°_n/90°_n)_s$ laminate. The 0° ply constraint upon the 90° is different for each of these laminates which is reflected in the dependency of the residual stress upon the m/n ratio, as shown in figure 27. In addition to the ply thickness, the stress required for the onset of transverse cracks in cross plied or angle plied laminates should depend also upon the material toughness as well as the mismatch of adjacent ply stiffnesses, [14 and 15], Poisson's ratios and coefficients of thermal expansion [15]. Therefore, a direct comparison between different material systems cannot be made. Moreover, it is believed that transverse cracking in virgin specimens, for a given material system and lay-up, should depend very strongly upon the curing, and cutting practice.

In general, any symmetric lay-up with transverse plies can be approximated by a cross plied lay-up of the form $(0'_m/90_n)_s$ where 0' is some equivalent group of smeared plies with reduced stiffness E_1'. In other words, the $(\pm30°_n/90°_{2n})_s$ lay-up used in the present work can be approximated to a cross plied laminate of m/n ratio equal to 1/2. If the stiffness of the ±30° plies in the $(\pm30°_n/90°_{2n})_s$ lay-up is somehow reduced, then the stress required to propagate transverse cracks will be increased. Such evidence can be found in figure 12 where the $(\pm30°_2/90°_4)_s$ laminate appears to have a larger density of transverse cracks when compared with the $(\pm30°_3/90°_6)_s$ or $(\pm30°_4/90°_8)_s$ laminates. If the ±30°

plies were uncracked in all sizes then one would expect the crack density to be progressively higher for thicker, virgin, laminates. However, the uncracked $\pm 30°_2$ plies in the $(\pm 30°_2/90°_4)_s$ impose a higher ply constraint upon the 90° plies than the cracked $\pm 30°_3$ or $\pm 30°_4$ plies in $(\pm 30°_3/90°_6)_s$ and $(\pm 30°_4/90°_8)_s$ laminates respectively. Thus, ply constraint and 90° ply thickness increase appear to have a similar influence upon transverse cracking.

As reported in the previous section, the modes of final failure in the fiber dominated lay-ups (**B** and **C**) depended upon the specimen size while the contrary was true for the two matrix dominated lay-ups (**A** and **D**). These transitions in the modes of final failure can be explained through the effect of transverse cracking upon the load bearing plies. For example, in the matrix dominated lay-up **A** final failure is largely controlled by the load bearing ±30° plies. In this case, the mode of final failure was more or less uniform in all four sizes because failure along the ±30° directions was the only alternative: no fibers could be broken. The effect of transverse cracking was merely reflected on the tensile strength. The large size specimens, in addition to the 90° ply cracks, suffered early cracking in the ±30° directions, as shown in figure 12, which effectively reduced the specimens' tensile strength.

For the fiber dominated lay-ups (**B** and **C**), the effect of matrix cracks was largely reflected in the mode of final failure, rather than in the tensile strength. For example, matrix cracks in the 90° plies of lay-up **B**, of the small size specimens, appeared to be responsible for promoting fracture in the load bearing 0° plies. In other words, transverse cracks in the 90° plies imposed a stress concentration upon the neighboring 0° plies. As a result, a clean 0°-ply fracture occured. It is believed that the difference in the mode of final failure, between the small and the large size specimens, lies in the decoupling rate between the 90° plies (source of stress concentrations) and the 0° plies (load bearing plies). Delamination in the large size specimens occurs at a much lower percentage of strength, as compared to the smaller size specimens. Hence, the 0° plies in the large size specimens can survive the local stress concentrations imposed by the transverse cracks in the 90° plies. Furthermore, the 45° plies which already contained cracks, as shown in figure 16, tend to delaminate

at a faster rate from the 0° plies. Thus, as the applied load increases, the chance of a localized fracture in the load bearing 0° plies is reduced.

In the case of the cross plied laminates (lay-up **C**), the presence of extensive matrix cracks between in the load bearing plies of the large size specimens effectively served as the decoupling mechanism, as delamination did in the quasi-isotropic laminates. Since the 0° plies of the large size specimens where badly split, a local fiber fracture could not have propagated transversely through the whole width of the 0° plies as it did in the case of the small size specimens, as shown in figure 9.

4.3 Strength

The ultimate objective of most research studies of this kind is to incorporate scaling effects into a failure criterion capable of predicting the strength of a full scale structure from laboratory generated data. Existing failure criteria for composite materials are empirical in nature and phenomenological, that is, the mode of failure cannot be predicted. In the case of brittle materials the strength of large structures can be predicted either from a fracture mechanics based model, like the one of Eq.3, or from a Weibull statistics based model, like the one of Eq.2. However, laminated composites are not truly brittle materials, in the sense that, cracks do not always propagate in a self-similar manner. Moreover, the tensile strength and the mode of failure of laminated composites depend upon factors unrelated to the volume or void concentration in a specimen. Such factors are stacking sequence, fiber diameter, fiber volume fraction, fiber/matrix interfacial strength, and ply thickness.

Tensile strength considerations, alone, suggest that ply-level scaling of composites becomes a major problem when a given lay-up is matrix dominated, such as lay-up **A** or **D**. Although not reported explicitly, a similar conclusion may be drawn from the results of Lagace *et al* [4]. Ply-level scaled laminates, with the same in-plane dimensions, were more sensitive to thickness increase when no 0° plies were present. In the same study, ply-level scaled laminates were more sensitive to thickness increase as compared to corresponding sub-laminate scaled laminates. However, Camponeschi [5] has reported an opposite effect in his study of the compressive strength of thick (48-192 plies)

composites, scaled at a sub-laminate level. His results suggest that unidirectional laminates were more sensitive to thickness increase than cross plied laminates. In agreement with the present findings, the strength of both lay-ups decreased with increasing laminate thickness.

Delamination is one of the most commonly observed damage mechanisms in laminated composites, and usually signals the end of life of such materials. Consequently, delamination has become a popular subject for research in the past 15-20 years. Some researchers have associated delamination to strength scaling effects [4 and 7]. The observed tensile strength reductions in specimens of a given lay-up with increased ply thicknesses have been attributed to edge stress effects which are responsible for causing delamination at lower applied loads. While this may be true for certain specific lay-ups and sizes, the generality of such an approach is questionable. In the present research work it has been shown that ply decoupling influences both the final failure mode as well as the strength of scaled laminated composites. However, such ply decoupling is not always associated with "pure" delamination as described by Lagace *et al* [4] or Rodini and Eisenmann [7]. As the ply thickness increases, transverse cracking becomes the primary, strength controlling mechanism and delamination is simply a secondary damage mode. Since ply decoupling depends upon the specimen size, as demonstrated by the modes of final failure, this will always be a strength controlling factor in scaled laminated composites, and has to be taken into account in the prediction of strength. Therefore, simple stand-alone strength prediction models based on volume of the material, free edge stress distribution, or the void size, are expected to be insufficient for general applications.

In many cases, a result of the same or similar degree of accuracy can be obtained from more than one method. Thus, the simplest models, like those of Eqs. 2 and 3, should be applied first. For example, Rodini and Einsmann [7], have combined the interlaminar normal stress distribution approach with Weibull statistics, and developed a model which predicts the stress at the onset of delamination. In addition, they have reported experimental results for scaled $(\pm 45°_n/0°_n/90°_n)_s$ laminates, where n=1, 2 and 3, tested at two temperature conditions, 75 °F and 250 °F. As shown in figure 29, the model of Eq.3 is in closer agreement with their experimental results than their more elaborate, model.

In the above example, the model given by Eq.3 yields a reasonable result, because delamination damage propagates in a self-similar fashion within the brittle phase of the composite material (the matrix). However, the successful application of Eq.3 to ultimate failure, and hence strength, depends upon the lay-up as shown in figure 30. For the purpose of direct comparison the ratio of the predicted to the measured strength, $S_{pred.}/S_{meas}$, was plotted, for each lay-up, versus the specimen size. Note that, the closer this ratio is to 1, the better the agreement between theory and experiment. It appears that, in general, the tensile strength of full scale size specimens, as predicted by Eq.3, is underestimated for all four lay-ups. From 9%, in the case of lay-up A, to as much as 47%, in the case of the cross plied lay-up D. The poor predictive capability of the model in the present problem is thought to be due to (a) the simplicity of equation Eq.3 (being related to size variations only) and (b) its limitation to brittle and homogeneous materials with some inherent voids or flaws.

A comparison between the Wiebull model, Eq.2 and the fracture mechanics based model, Eq.3 is shown in figure 31. The shape parameter m was evaluated for each lay-up from the two smallest sizes. Note that, for both the 1/4 and the 2/4 scale sizes, $S_{pred.}/S_{meas.}$ is equal to 1, hence, the 1/4 scale size has being omitted from figure 31. Since the model of Eq.2 involves an empirically obtained parameter, its predictive capability appears to be much better than that of Eq.3. Unlike the strength predictions of Eq.3, the strength predicted by Eq.2 has been overestimated in all four lay-ups. In particular, the strength of the full scale specimens of lay-up D has been overestimated by as much as 18%. This overestimate can be attributed to the shape parameter m which was evaluated from the 1/4 and 2/4 scale size specimens. For lay-up **D**, these two sizes, unlike the 3/4 and 4/4 scale size specimens, were uncracked prior to testing. On the contrary, in the case of lay-up A, only one of the two specimens used to calculate the shape parameter m, was cracked. Thus, the strength of the full scale size specimens, in this case, was predicted within 2.5%. Clearly, the parameter m is a function of the initial state of the specimen and a function of how the initial state affects the ultimate mode of failure.

Obviously, the predictive performance of Eq.2 will depend on a correct estimate for the shape parameter m which depends upon the uniformity of the material's internal micro or macro structure as the specimen size increases. Note that, the word uniformity refers to any material changes that may have a positive or negative effect on strength. For example, transverse cracks were present in approximately equal amounts in both lay-ups **D** and **C**. The ±45° cracks present in lay-up **D** had a negative effect on the strength scaling of that laminate. For lay-up **C**, on the other hand, the negative effect due to the 90° ply cracks was offset by the simultaneous development of 0° transverse cracks (which effectively led to ply decoupling, a positive contribution to tensile strength). Thus, as shown in figure 31, the full scale strength of lay-up **C** was predicted correctly within 3.7% as opposed to 18% for lay-up **D**. The mode of final failure in the quasi-isotropic specimens suggested that some degree of ply decoupling did take place. However, unlike the cross plied lay-up, the strength of the quasi-isotropic laminates depends upon the integrity of the 0° plies as well as the integrity of the ±45° plies (which make up 50% of the laminate). Thus, as one would expect, the predictive accuracy of the full scale strength of the quasi-isotropic lay-up lies half way between that of the cross plied and the $(\pm 45°_4/\pm 45°_4)_s$ lay-up.

Popular failure theories and criteria which are usually employed in the design of simple composite structures are: the maximum stress or strain theories, the Tsai-Hill, and the Tsai-Wu criteria [13]. Each one of these are extensions of isotropic material theories to orthotropic materials, and their basic purpose is to curve fit available experimental data. Therefore, a measure of performance of a given failure criterion is the degree of correlation between theory and experiment.

The maximum stress and strain theories can be referred to as five in one failure criteria since ply failure is deemed to occur when one or more of the five ply strengths is exceeded. These are the longitudinal tensile and compressive, the transverse tensile and compressive, or the shear strengths. Failure theories of this type are relatively easy in their application provided that the five (or at least three) independent ply strengths or strains to failure are known. Their application, then, consists of the simultaneous solution of three or more inequalities for each ply in a composite laminate. The

result is the minimum load required to cause a first ply failure. Note that axial, transverse, and shear failures are presumed to occur independently.

Another failure theory for composites can be obtained from a modified Von Mises' yield criterion for isotropic materials where the yield strengths are substituted by ply strengths. Thus, the failure criterion reduces to Eq.4 for a unidirectional ply, where the subscript 1 denotes the fiber direction, and 2 the the transverse direction (see Jones [13]).

$$\frac{\sigma_1^2}{S_1^2} - \frac{\sigma_1\sigma_2}{S_1^2} + \frac{\sigma_2^2}{S_2^2} + \frac{\tau_{12}^2}{S_{12}^2} = 1 \tag{4}$$

S_1, S_2, and S_{12} are the ply longitudinal, transverse, and shear strength respectively. Likewise, σ_1, σ_2, and τ_{12} are the the applied stresses. With the introduction of the stress transformation equations, for uniaxial loading:

$$\sigma_1 = \sigma_x\cos^2\theta,\ \ \sigma_2 = \sigma_x\sin^2\theta \ \text{ and } \tau_{12} = -\sigma_x\sin\theta\cos\theta \tag{5}$$

the criterion applied to any off-axis ply becomes:

$$\frac{\cos^4\theta}{S_1^2} + \left(\frac{1}{S_{12}^2} - \frac{1}{S_1^2}\right)\cos^2\theta\sin^2\theta + \frac{\sin^4\theta}{S_2^2} = \frac{1}{\sigma_x^2} \tag{6}$$

Eq.6 is known as the Tsai-Hill failure criterion. A major advantage of this criterion over the maximum stress or strain failure theories is the fact that a system of inequalities is replaced by a single equality. In other words, the different strengths of a ply (axial, transverse and shear) are coupled through a single equation. However, like the other two, the Tsai-Hill criterion is only capable of predicting first ply failure. Therefore, its usefulness is restricted to single ply composites.

A more advanced failure theory is the Tsai-Wu tensor theory. In this theory the curve fitting performance is improved by the addition of another experimentally obtained parameter. This parameter results from the interaction between stresses in a biaxial stress system and is referred to as the interaction strength, denoted by F_{12}:

$$F_{12} = \frac{1}{2\sigma^2}\left[1 - \left(\frac{1}{S_1^t} + \frac{1}{S_1^c} + \frac{1}{S_2^t} + \frac{1}{S_2^c}\right)\sigma + \left(\frac{1}{S_1^t S_1^c} + \frac{1}{S_2^t S_2^c}\right)\sigma^2\right] \tag{7}$$

where $S^t{}_1$, $S^c{}_1$ etc are the tensile and compressive strengths, respectively, of a unidirectional ply in the 1 direction and σ is the biaxial tensile failure stress. Thus, F_{12} can be evaluated if the strengths of a ply and σ are known, see Jones [13]. Furthermore, Tsai [9] defines a normalized interaction strength, $F^*{}_{12}$, and a strength ratio R which are given by:

$$F_{12}^* = F_{12}\sqrt{S_1^t S_1^c S_2^t S_2^c} \text{ and } R = \frac{\{\sigma\}_{max}}{\{\sigma\}_{appl}} \tag{8}$$

where $\{\sigma\}_{max}$ is the ultimate stress and $\{\sigma\}_{appl}$ is the applied stress. When the strength ratio R = 1, failure occurs. Assuming plane stress conditions, the strength ratio R, for a given ply, can be obtained from the quadratic equation:

$$(F_{12}\sigma_1\sigma_2)R^2 + (F_1\sigma_1)\,R - 1 = 0 \tag{9}$$

where σ_1, σ_2 are the applied stresses and F_{12}, F_1 are related to ply strengths. Eq.9 is known as the quadratic criterion. This criterion, like others, is applied to each ply within a composite laminate. Consequently, the ply with the lowest strength ratio will fail first and this is known as the first ply failure. This failure, in most cases, consists of transverse matrix cracking parallel to the fiber orientation. Successive failure then proceeds until the ultimate failure, known as the last ply failure, occurs. Such successive ply failure may be accounted for by the introduction of a matrix degradation factor, [9], which is a measure of how fast the plies are degraded by matrix cracking. The quadratic criterion, when used in conjunction with the matrix degradation factor, appears to be one of the most powerful tools for strength prediction. Therefore, it has been employed in the present study to assess its applicability to scaled composite laminates. Strength predictions by the quadratic criterion were obtained with the aid of a commercially available computer program "GenLam", [9], and are presented in table 4. For these strength predictions, the value for $F^*{}_{12}$ was chosen as -0.5; since no known measured value for AS4/3502 was available at the time of calculation. Note that a value of $F^*{}_{12}$, for AS/3501, equal to -0.5 is reported by Tsai [9]. Other input values (for ply strengths) used

in the calculation are shown in tables 5 and 6. In addition, it has been assumed that the temperature difference between the stress free state and the operating temperature is -180 °F.

For comparison, the experimentally obtained strengths corresponding to the 1/4 scale size specimens are included also in Table 4. It is clear that the correct prediction of strength, for a given set of input data, depends upon the correct choice of the degradation factor, D.F.. Note that when a single value for D.F. is used, for example 0.2 which is a value recommended for AS/3501 by Tsai [9], the model fails to predict the strength of at least one of the four lay-ups. Overestimates of 217% and 119% have been obtained in the case of lay-up A when input values from tables 5 and 6 respectively were used. The large discrepancy in strength is a result of a combination of several factors, including inaccurate ply strength data, inaccurate values for the empirical constant F^*_{12} and the D.F., and ply thickness effects. The 1/4 size specimen of lay-up A had the largest number of concentrated plies in comparison with the other three lay-ups: four in lay-up A as opposed to two in the other three lay-ups. The result of such large ply thickness meant that matrix cracks could initiate at low applied load thus, a greater degradation factor should be used. It would appear that a reasonable agreement between theory and experiment could be obtained with a value of D.F = 0.3, for lay-ups B, C and D, and a value of 0.7 for lay-up A. In other words, since the degradation factor is a measure of how fast the plies are degraded by matrix cracking, this factor should also be a function of ply thickness, as demonstrated by the results in table 4.

Clearly, the quadratic criterion can predict the ultimate strength of laminated composites, but size effects such as the effect of thickness upon strength cannot be handled. If, for a given family of scaled specimens, the matrix degradation factor is kept constant, the failure model cannot predict the reduction in strength due to the increase in specimen size. Since pre-existing cracks in the thick plies, of the large size specimens, were partially responsible for the observed strength reductions, it would be reasonable to suggest that a full scale size strength prediction may be achieved by introducing a varying matrix degradation factor. In other words, it might be possible to find an empirical relationship between the matrix degradation factor and specimen size. Even though the suggestion is

reasonable, it is demonstrated in figure 32 that the predicted strength is not only a function of the matrix degradation factor, but also depends upon the lay-up. For example, while the $(\pm 45°/\pm 45°)_s$ lay-up was shown to be very sensitive to size effects in measured strength, the predicted strength using the quadratic criterion appears to be insensitive to matrix degradation factor changes, as shown in figure 32. The predicted tensile strength of lay-up C, however, appears to be a strong function of the D.F. even though this laminate exhibited the least size sensitivity experimentally. Since there is no straight forward relationship between the D.F. and specimen size, this failure criterion cannot be used as suggested.

An alternative approach might be to use the quadratic failure criterion in conjunction with other models capable of handling size effects, such as the ones described by Eqs.2 and 3: since the ply strengths, $S^t{}_1$, $S^t{}_2$ and S_{12}, of a composite unidirectional ply may be expected to decrease with increasing size, appropriately predicted strengths and stiffnesses corresponding to the full scale size structure can be used as inputs for the quadratic failure criterion. The full scale strength $S^t{}_1$ could be predicted reasonably accurately from a simple model such as that of Eq.2, provided that material uniformity can be achieved during fabrication: since, a unidirectional composite will be residual stress free, at least within the boundaries of practically useful ply thicknesses, there is no reason to suggest otherwise. Likewise, the full scale ply strength $S^t{}_2$ could be predicted from Eq.3. Due to the fiber constraint, final failure can take place only in the transverse direction, at a single location within the gage length, from a self-similar crack propagation. Thus, the fracture mechanics based model of Eq.3 should be the most appropriate. Furthermore, it may be assumed that, the full scale shear strength could be predicted from the full scale tensile strength, $S_{(\pm 45)}$, of the $(\pm 45°_n/\pm 45°_n)$ laminates where,

$$S_{12} = \frac{S_{(\pm 45°)}}{2} \tag{10}$$

However, as shown in figure 31, the prediction of the full scale strength of the $(\pm 45°_4/\pm 45°_4)_s$, $S_{(\pm 45°)}$, is unsatisfactory. In this case, a different empirical best fit curve, such as the simple straight line, Eq.11, may be more appropriate.

$$S_f = S_m(1.12 - 0.12\lambda) \tag{11}$$

where S_f and S_m are the strengths of the full scale and model specimens respectively. Combining Eqs.10 and 11, a relationship between the model and full scale shear strengths, Eq.12, can be obtained:

$$S^f_{12} = S^m_{12}\left(1.12 - 0.12\lambda\right) \tag{12}$$

The new full scale ply strengths, calculated from Eqs. 2, 3 and 12 (for λ=4), are shown in table 7. For Eq. 2, the value for the shape parameter m = 10.5, for the unidirectional strength, was obtained from flexure test results, AS4/3502, reported by Jackson [11].

The full scale strength for each lay-up has been obtained by the application of the quadratic criterion in conjunction with the full scale ply properties given in table 7. The predicted full scale strengths from the three methods, the combination model, Eq.2, and Eq.3 are listed together with the experimentally obtained full scale strength values in table 8. Note that in the case of the combination model it has been assumed that only S^t_1, S^t_2 and S_{12} will have any significant effect upon the tensile strength. In other words, the size effect upon the ply stiffnesses and the compressive strengths (S^c_1, S^c_2) are neglected. Furthermore, the value for the D.F. was chosen according to the best match results in table 4. It is clear, from the results of table 8, that the Weibull statistics based model provides the best strength prediction. However, it has to be pointed out that the successful application of the combination model to the scaling problem depends very strongly upon the correct choice of initial ply properties. Simple as this may appear to be, published results of ply strengths, for the same material system, varied by as much as 33.3% and 52.7% for tension and compression respectively, as shown in tables 5 and 6.

4.3 Failure Strain

The failure strain was found to be much more sensitive to the method of measurement as compared to strength. Furthermore, results showed that there was no simple correlation between the failure strain, the type of lay-up, and the specimen size. For lay-ups **A**, **C** and **D**, the failure strains tend to increase with decreasing specimen size; however, an opposite effect was observed in the case of lay-up **B**. It would seem appropriate, therefore, to conclude that the sensitivity of the failure strain on the specimen size depends on the stacking sequence as well as the lay-up and the method of measurement.

Theoretically, strain based failure criteria have an advantage over stress based criteria since strains in the longitudinal and transverse directions are coupled directly. Conversely, the stresses in most failure theories are considered to be independent, [16]. However, the correct application of strain based criteria require ply strains to failure to be measured experimentally. Results from the present study show that such measurements are sensitive to the type of method used. Therefore, additional and sometimes substantial errors can be incorporated into such criteria. It has also been suggested, [9], that the strain to failure may be obtained from strength and stiffness values. Clearly such an approach can only be applied to composites which exhibit quasi-linear stress/strain behavior. Figure 33, shows a relative decrease in strength with specimen size for all four lay-ups whereas, figure 34 shows that a similar behavior does not exist in the case of the failure strain. Clearly, if the initial stiffness and strength values were to be used to predict the failure strain, a very large error would occur.

In this study all four chosen lay-ups had off-axis plies on the outer surface, which meant that strain gages attached to those surfaces would be incapable of measuring the maximum strain to failure due to damage. In contrast, the extensometers exhibited a relatively more consistent behavior, although some slipping did occur, especially for specimens with badly cracked surface angle-plies.

4.4 Stiffness

In addition to design considerations, understanding of scaling effects becomes important when standard methods have to be specified. The measured strain to failure by the various methods used and the theoretical predictions by lamination theory are presented in table 3. These results suggest that for small strains, and within an experimental error, the stiffness is independent of the method of measurement as well as the specimen size. Furthermore, lamination theory tends to provide an acceptable agreement with experiment with the best match occurring in lay-up **D** and the worst in lay-up **A**. The fact that experiment and lamination theory are approximately 25% apart, in the case of lay-up **A**, may be attributed to the extensive matrix damage associated with this lay-up due to ply grouping. This particular lay-up had the largest number of grouped plies, compared to the other three lay-ups.

The complete stress/strain behavior, which is presented in figures 3-6 for lay-ups **A** - **D** respectively, shows that, as the strain increases, the stress/strain response becomes sensitive to both the method of measurement as well as the specimen size. For example, a significant loss in stiffness takes place in specimens of lay-up **A** at a stress of just over 20 ksi in the 2/4 size specimens. The X-ray radiographs of figure 20 show that this applied stress is associated with the initiation of delamination. Note, in figure 3, that a slight stiffness reduction has occurred in the 1/4 size specimens at a higher load.

An interesting deviation of the stress/strain curve has occurred also in the large size specimens of lay-up **B**, figure 4. The deviation was registered by the extensometers alone and was later associated with the initiation of edge delamination, see figure 16. This is an important observation since it demonstrates the limitation of small gage length strain measuring sensors. In general, global effects which may significantly alter the specimens elastic behavior, cannot be registered by local strain measuring devices, unless of course the sensor (strain gage in this case) happens to be located in the vicinity of the damage.

Contrary to the strain gage reading, the extensometers registered a marginal increase in stiffness in the largest size specimens of lay-up **A** and **D** as shown in figures 3 and 6. These two lay-ups contained angle-plies on the outside. The only possible explanation for this behavior is knife edge slipping due to surface ply in-plane rotation. The heavily cracked outer plies, in the full scale specimens (figures 15 and 19), have a tendency to align themselves with the loading direction as the applied load increased.

One of the standard methods of measuring the shear stiffness of composites consists of the tensile testing of (±45°) laminates. The experimental results from the present work show that the Stress/strain behavior of this type of laminate depends upon the method of measurement as well as the ply thickness, figure 6, with strength and strain to failure being affected the most. Thus, a more careful study of the influence of ply thickness upon the strength and stiffness as well as the adequacy of the instrumentation is needed.

5. CONCLUSIONS

5.1 Damage

Damage development and the final mode of failure were found to be size sensitive. It was observed that the degree of size sensitivity depended upon the lay-up. The two matrix dominated lay-ups **A** and **D** showed the least dependence upon scaling size. In contrast, modes of final failure, in the fiber dominated lay-ups, **B** and **C**, were more sensitive to size effects. It has been shown that matrix damage in virgin specimens has contributed to the observed behavior. Such damage often led to ply decoupling, which is not necessarily synonymous with the word "delamination". The rate of ply decoupling was the most important factor in controlling the mode of final failure and consequently, the ultimate strength of the laminate.

While triggering of the transverse crack initiation is thought to have resulted from cutting, the actual driving mechanism is thought to have been a result of the residual stresses. According to both Weibull and fracture mechanics based models, residual stresses have a more detrimental effect upon the thickest plies, making it possible for transverse cracks to initiate in thick virgin laminates.

5.2 Strength

So far as strength is concerned all four lay-ups were found to be scale size sensitive. The degree of sensitivity was very much dependent upon the given lay-up. An 83% increase in strength was observed in 1/4 size specimens, of the matrix dominated lay-up **A**, as compared to the full scale size specimens. In contrast, the average strength of the 1/4 size specimens of the fiber dominated lay-up C, was only 7% higher than the average strength of full scale specimens.

Prediction of the full scale strength has been attempted by the use of three approaches:

(a) a Weibull statistics based model, Eq.2,

(b) a fracture mechanics based model, Eq.3 and,

(c) a combination model involving Eqs.2 and 3 in conjunction with the quadratic failure criterion, described by Tsai [9].

A comparison with the experimental findings showed that the predicted full scale strength was overestimated by method (a), for all lay-ups, while methods (b) and (c) predicted a lower than measured full scale strength. The best full scale strength predictions were obtained from the first method, which is thought to be the most appropriate to the scaling problem.

It has been shown that the predictive performance of the Weibull statistics based model depends upon the material uniformity with increasing size. The more uniform a material is the better the extrapolated full scale strength. Recommendations for improvements of this method have also been suggested.

Application of the quadratic failure criterion indicated that a successful prediction in strength, for a given specimen size, can be obtained provided that a suitable value for the degradation factor is used. Furthermore, it has been shown that the degradation factor is a function of the ply thickness for a given lay-up: it is not a material constant.

5.3 Failure Strain

The failure strain was found to be sensitive to the method of measurement. Furthermore, results showed that there was no simple correlation between the failure strain, the type of lay-up and the specimen size. Although in most cases (lay-ups **A**, **C** and **D**) the failure strains tend to increase with decreasing specimen size, an opposite effect was observed for lay-up **B**.

Due to difficulties associated with the measurement of failure strain it is concluded that a failure criterion based upon stress would be a better choice.

5.4 Stiffness

For small strains the stiffness values appeared to be independent of specimen size as lamination theory would predict. However, at large strain values the stiffness depended upon both the specimen size as well as the method of measurement. It has been shown that the stress/strain behavior can be correlated to observed damage mechanisms, provided that an appropriate method of measurement is used.

6. SUGGESTED FURTHER WORK

It has been observed that the strength and the stress/strain behavior was highly influenced by damage which in many cases preexisted in virgin specimens. It is thought that a better understanding of the relationship between matrix cracks, stacking sequence, matrix toughness, strain to failure of the 90° plies, and ply relative stiffnesses is needed. Such a relationship can be obtained by careful monitoring of the stress required to initiate the cracks. From these tests, a Weibull or fracture mechanics based model can be adopted to the crack initiation problem.

So far as the failure criteria are concerned, it is suggested that values of ply strength and stiffness be experimentally obtained for each and every material system to be evaluated in the future. At least two sizes of specimens need to be tested to obtain true values for the shape parameter. In addition, the value of the normalized interaction strength, F^*_{12}, has to be experimentally obtained for every material system for the successful application of the combination model.

It has been shown that the ply thickness rather than the material volume may be be a more appropriate scaling factor. This observation, which may have a considerable effect upon the successful development of an adequate failure criterion, has to be verified experimentally. It is suggested that identical tests be performed on thickness rather than volume scaled specimens. If the same degree of size effect in strength is achieved in both the thickness and volume scaled specimens, then the problem of size could be attributed conclusively to the effect of ply thickness alone.

Based upon published results, it appears that sublaminate scaling is an option that must be considered in conjunction with ply-level scaling. Therefore, it is suggested that future scaling work should involve laminates, scaled at both levels, as well as different material systems, including a comparison between thermoset and thermoplastic systems.

REFERENCES

[1] Zweben C. "The effect of stress nonuniformity and size on the strength of composite materials", Composites Technology Review, Vol.3, No.1, 1981.

[2] Kaminski B.E."Effects of specimen geometry on the strength of composite materials", ASTM STP 521, 1973.

[3] Morton J. "Scaling of impact-loaded carbon-fiber composites", AIAA Journal, Vol.26, No.8, 1988.

[4] Lagace P., Brewer J., and Kassapoglou C., "The effect of thickness on interlaminar stresses and delamination in straight-edged laminates", Composite Technology Review, 1989.

[5] Camponeschi E.T., Jr., "Compression testing of thick-section composite materials", David Taylor Research Center, Ship Materials Engineering Dept., Research & Development Report, DTRC-SME-89/73 October 1989.

[6] Batdorf S.B., "Note on composite size effects", Journal of Composites Technology & Research, Vol.11, No.1, 1989.

[7] Rodini B.T. and Eisenmann, J.R., "An analytical and experimental investigation of the edge delamination in composite laminates", Fibrous Composites in Structural Design, E.M. Lenoe, Ed., Pleum Press, NY, 1978.

[8] Atkins A.G. and Caddell R.M., "The laws of similitude and crack propagation", International Journal of Mechanics Science, Pergamon Press, Vol.16, 1974.

[9] Tsai S.W., "Composites design, 4th edition", Think Composites, Dayton Ohio, 1988.

[10] Wang A.S.D. "Fracture mechanics of sublaminate cracks in composite materials", Composites Technical Review, 6:45, 1984.

[11] Jackson K.E., "Scaling effects in the static and dynamic response of graphite-epoxy beam-columns", PhD Thesis, Engineering Science and Mechanics Dept., Virginia Polytechnic Institute and State University, Blacksburg VA, 1990.

[12] Highsmith A.L. and Reifsnider K.L. "Stiffness reduction mechanisms in composite laminates", ASTM STP 775, 1983.

[13] Jones R.M., "Mechanics of composite materials", Hemisphere Publishing Corporation, NY, 1975.

[14] Bader M.G., Bailey J.E., Curtis P.T. and Parvizi A., "The mechanisms of initiation and development of damage in multi-axial fibre-reinforced plastic laminates", Mechanical Behaviour of Materials, Proceedings ICM 3, Vol.3, 1979.

[15] Chan W.S. and Wang A.S.D., "A study on the effects of the 90° ply on matrix cracks in composite laminates", Structures, Structural Dynamics and Materials Conference, 27th, San Antonio, TX, May 1986.

[16] Hart-Smith L.J., "A new approach to composite laminate strength prediction" Douglas Paper 8366, Presented to MIL-HDBK-17 Committee Meeting, Riviera Beach, Florida, 1989.

Table 1. Specimen geometric details.

	1/4 SIZE	2/4 SIZE	3/4 SIZE	FULL SCALE
No. of plies	8	16	24	32
Average thickness in.x10^{-3}	44	88	133	176
Nominal width in.	0.5	1.0	1.5	2.0
Nominal gage length / in.	3.5	7.0	10.5	14.0
Nominal gripped length / in.	0.75	1.50	2.25	3.00
No. of specimens	22	10	12	10

Table 2. Summary of the Experimental strength and failure strain results: average values from six or more valid tests per condition.

SIZE	TENSILE STRENGTH ksi	FAILURE STRAIN %	NORMALIZED STRENGTH	NORMALIZED STRAIN
		Lay-Up **A** $(+30°_n/-30°_n/90°_{2n})_s$		
1/4	30.28	0.60	1.83	1.88
2/4	22.70	0.55	1.37	1.74
3/4	19.01	0.33	1.15	1.04
full scale	16.58	0.32	1.00	1.00
		Lay-Up **B** $(+45°_n/-45°_n/0°_n/90°_n)_s$		
1/4	80.78	1.20	1.39	0.82
2/4	72.35	1.18	1.24	0.81
3/4	61.97	1.42	1.06	0.97
full scale	58.34	1.47	1.00	1.00
		Lay-Up **C** $(90°_n/0°_n/90°_n/0°_n)_s$		
1/4	128.26	1.38	1.07	1.48
2/4	126.56	1.17	1.05	1.26
3/4	125.58	1.25	1.04	1.34
full scale	120.42	0.93	1.00	1.00
		Lay-Up **D** $(+45°_n/-45°_n/+45°_n/-45°_n)_s$		
1/4	19.63	1.05	1.56	2.49
2/4	17.08	0.96	1.36	2.29
3/4	14.96	0.74	1.19	1.77
full scale	12.56	0.42	1.00	1.00

Table 3. Summary of the longitudinal initial stiffness. Values shown represent the average of six or more extensometer tests. Stiffness values are valid for small strains: 0.2%, 0.5%, 0.5%, and 0.35% strain for lay-ups **A**, **B**, **C**, and **D** respectively.

	INITIAL STIFFNESS / Msi			
SIZE	EXTENSOMETER	CENTRAL GAGES	EDGE GAGE	LAMINATION THEORY* **T5 / T6**
		Lay-Up **A** $(+30°_n/-30°_n/90°_{2n})_s$		
1/4	5.1	5.4	5.5	6.7 / 6.4
2/4	5.2	5.3	5.6	6.7 / 6.4
3/4	5.2	5.1	4.8	6.7 / 6.4
full scale	6.1	5.0	4.9	6.7 / 6.4
		Lay-Up **B** $(+45°_n/-45°_n/0°_n/90°_n)_s$		
1/4	6.8	7.0	7.1	8.1 / 7.8
2/4	6.8	6.8	7.2	8.1 / 7.8
3/4	/	/	/	8.1 / 7.8
full scale	6.5	6.4	7.0	8.1 / 7.8
		Lay-Up **C** $(90°_n/0°_n/90°_n/0°_n)_s$		
1/4	9.4	9.8	/	11.2 / 10.7
2/4	10.2	10.0	/	11.2 / 10.7
3/4	/	/	/	11.2 / 10.7
full scale	/	/	/	11.2 / 10.7
		Lay-Up **D** $(+45°_n/-45°_n/+45°_n/-45°_n)_s$		
1/4	2.2	2.4	2.4	2.7 / 2.9
2/4	2.4	2.5	2.6	2.7 / 2.9
3/4	2.4	2.4	2.2	2.7 / 2.9
full scale	2.8	2.4	2.2	2.7 / 2.9

* The two independent sets of ply properties used in the theoretical stiffness predictions can be found in table 5, **T5**, and table 6, **T6**.

Table 4. Comparison of measured and calculated tensile strengths. The material mechanical properties used, are listed in tables 5 and 6.

	STRENGTH ksi					
	EXPERIMENT	QUADRATIC CRITERION (F^*_{12} = -0.5)				
LAY-UP	1/4 Size	D.F.= 0.2 T4* / T5*	D.F.= 0.3 T4	D.F.= 0.5 T4	D.F.= 0.7 T4	D.F.= 1.0 T4
$(\pm 30/90_2)_s$	30.3	96.1 / 66.4	75.5	44.3	29.8	18.5
$(\pm 45/0/90)_s$	80.8	97.7 / 65.7	83.6	51.8	34.8	21.0
$(90/0)_{2s}$	128.3	131 / 88.2	129.1	78.6	49.5	28.2
$(\pm 45)_{2s}$	19.6	21.9 / 24.5	21.0	19.4	17.6	14.8

* Stand for Table 4 and table 5 respectively.

Table 5. Material properties used for strength and stiffness prediction. These represent average values from four data sheets supplied by the manufacturer. The coefficients of thermal expansion were not supplied: AS4/3501 values reported in [9] were used.

ELASTIC CONSTANTS	COEFFICIENTS OF THERMAL EXPANSION	TENSILE AND SHEAR STRENGTHS	COMPRESSIVE STRENGTHS
E_1 =20.55 Msi	$\alpha_1 = -0.17 \times 10^{-6}/°F$	S^t_1 =267.7 ksi	S^c_1 =280.0 ksi
E_2 = 1.77 Msi	$\alpha_2 = 15.60 \times 10^{-6}/°F$	S^t_2 = 8.9 ksi	S^c_2 = 30.0 ksi
G_{12}= 0.77 Msi	/	S_{12}= 11.5 ksi	/
ν_{12} = 0.30	/	/	/

Table 6. Material properties used for strength and stiffness prediction. These values were reported in [11]. The coefficients of thermal expansion were not supplied: AS4/3501 values reported in [9] were used.

ELASTIC CONSTANTS	COEFFICIENTS OF THERMAL EXPANSION	TENSILE AND SHEAR STRENGTHS	COMPRESSIVE STRENGTHS
E_1 =19.85 Msi	$\alpha_1 = -0.17 \times 10^{-6}/°F$	S^t_1 =178.1 ksi	S^c_1 =132.4 ksi
E_2 = 1.43 Msi	$\alpha_2 = 15.60 \times 10^{-6}/°F$	S^t_2 = 7.5 ksi	S^c_2 = 32.3 ksi
G_{12}= 0.82 Msi	/	S_{12}= 12.5 ksi	/
ν_{12} = 0.29	/	/	/

Table 7. Material properties used for the full scale strength prediction. Calculations for Strength were based on initial values according to Table 5.

ELASTIC CONSTANTS	COEFFICIENTS OF THERMAL EXPANSION	TENSILE AND SHEAR STRENGTHS	COMPRESSIVE STRENGTHS
E_1 =20.55 Msi	$\alpha_1 = -0.17 \times 10^{-6}/°F$	S^t_1 =180.1 ksi	S^c_1 =280.0 ksi
E_2 = 1.77 Msi	$\alpha_2 = 15.60 \times 10^{-6}/°F$	S^t_2 = 4.5 ksi	S^c_2 = 30.0 ksi
G_{12}= 0.77 Msi	/	S_{12} = 7.4 ksi	/
ν_{12} = 0.30	/	/	/

Table 8. Strength predictions for the full scale specimens

	STRENGTH ksi			
LAY-UP	EXPERIMENT (4/4 Size)	COMBINATION MODEL	$\frac{S^{ult}_{1/4}}{S^{ult}_{4/4}} = \left(\frac{V_{4/4}}{V_{1/4}}\right)^{\frac{1}{m}}$	$S^{ult}_{4/4} = \frac{S^{ult}_{1/4}}{\sqrt{\lambda}}$
$(\pm 30/90_2)_s$	16.6	7.6 (D.F.=0.7)	17.0	15.1
$(\pm 45/0/90)_s$	58.3	41.4 (D.F.=0.3)	64.7	40.4
$(90/0)_{2s}$	120.4	60.5 (D.F.=0.3)	124.9	64.1
$(\pm 45)_{2s}$	12.6	9.4 (D.F.=0.5)	14.8	9.8

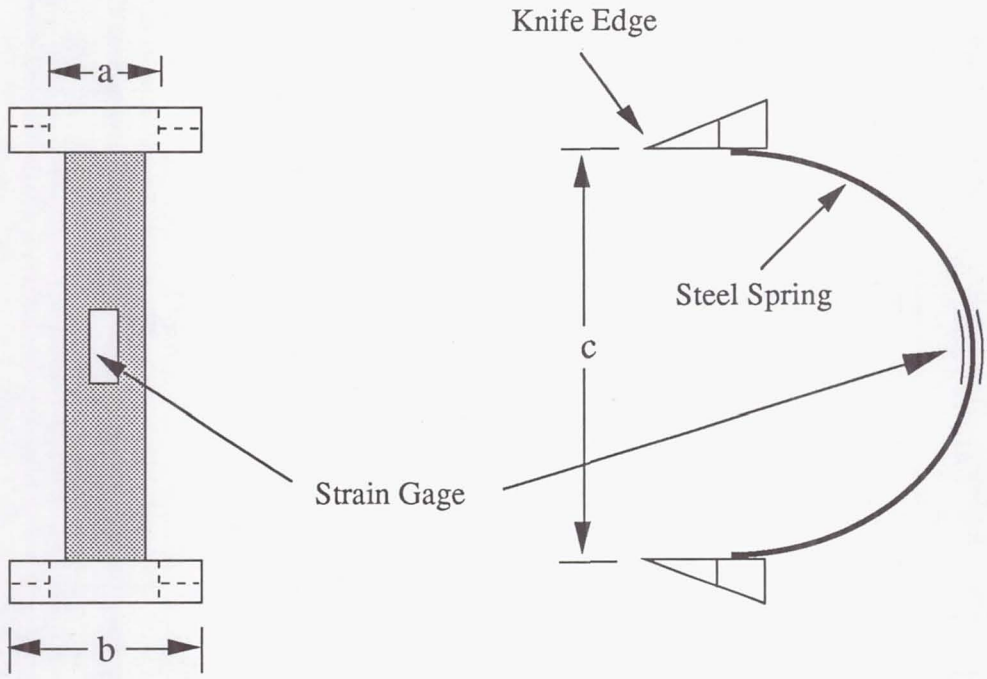

Fig.1 Custom built extensometers. The dimensions a, b, and c for the different specimen sizes were: a =1/3", 2/3", 3/3", 4/3"; b = 3/4", 5/4", 7/4", 9/4" and; c =3/2", 3," 9/2", 6" for scale size 1/4, 2/4, 3/4 and full scale size respectively.

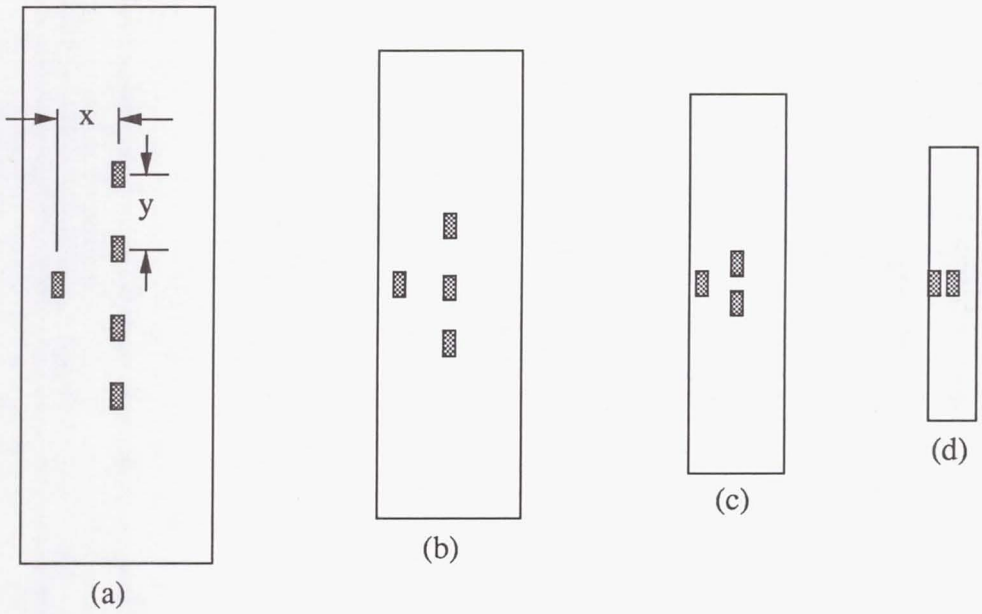

Fig.2 Strain gage instrumented specimens. The number and position of the gages were determined by the size of the specimen. The dimension x was equal to 12/16", 9/16", 6/16", and 3/16" for (a), (b), (c), and (d) respectively. The dimension y was equal to 3/2", 2/2" and 1/2" for (a), (b), and (c) respectively.

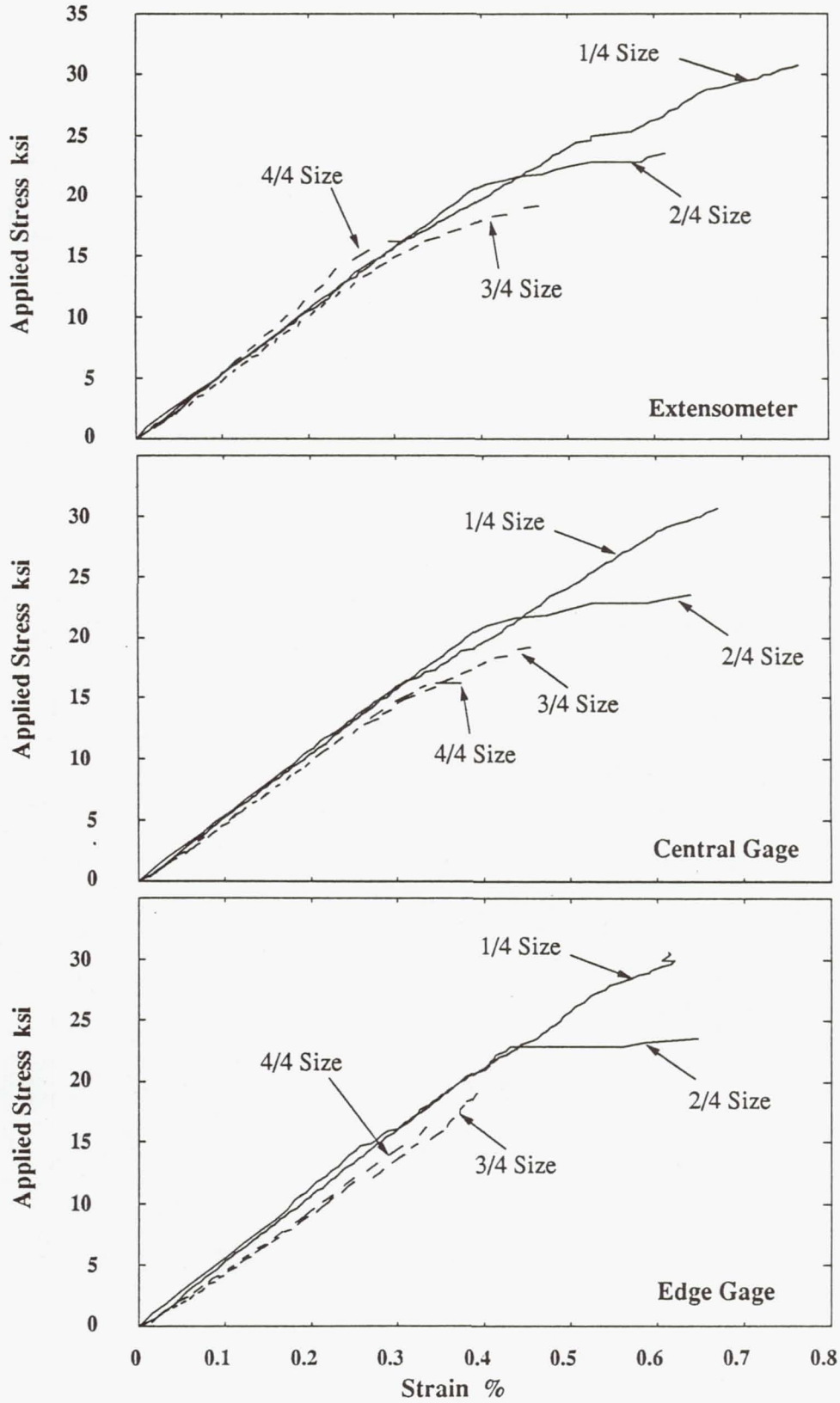

Fig.3 Stress/strain response for lay-up **A**. The strain was measured in three different ways: (a) with an extensometer, (b) with a series of centrally located strain gages, and (c) with one strain gage located close to the edge.

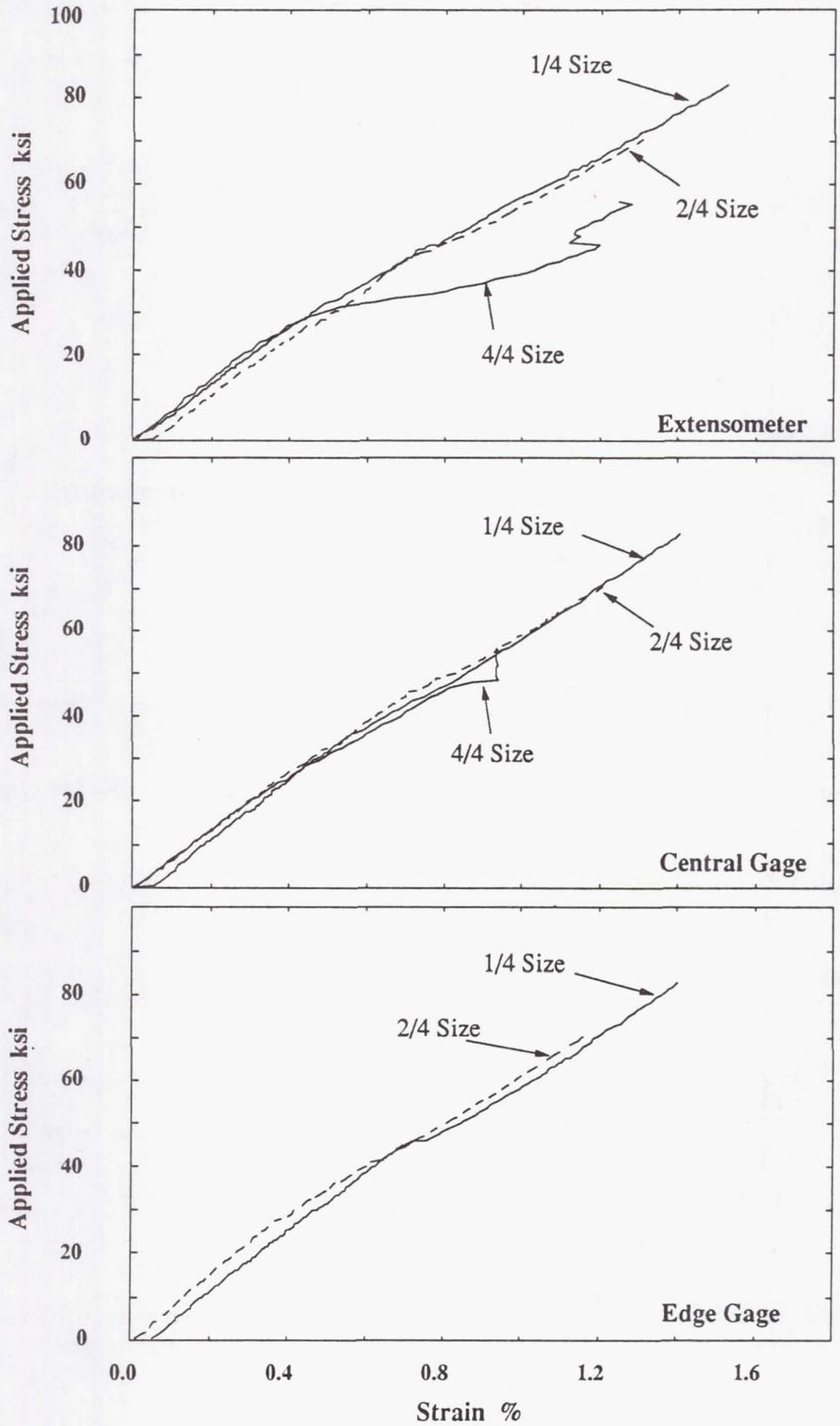

Fig.4 Stress/strain response for lay-up **B**. The strain was measured in three different ways: (a) with an extensometer, (b) with a series of centrally located strain gages, and (c) with one strain gage located close to the edge.

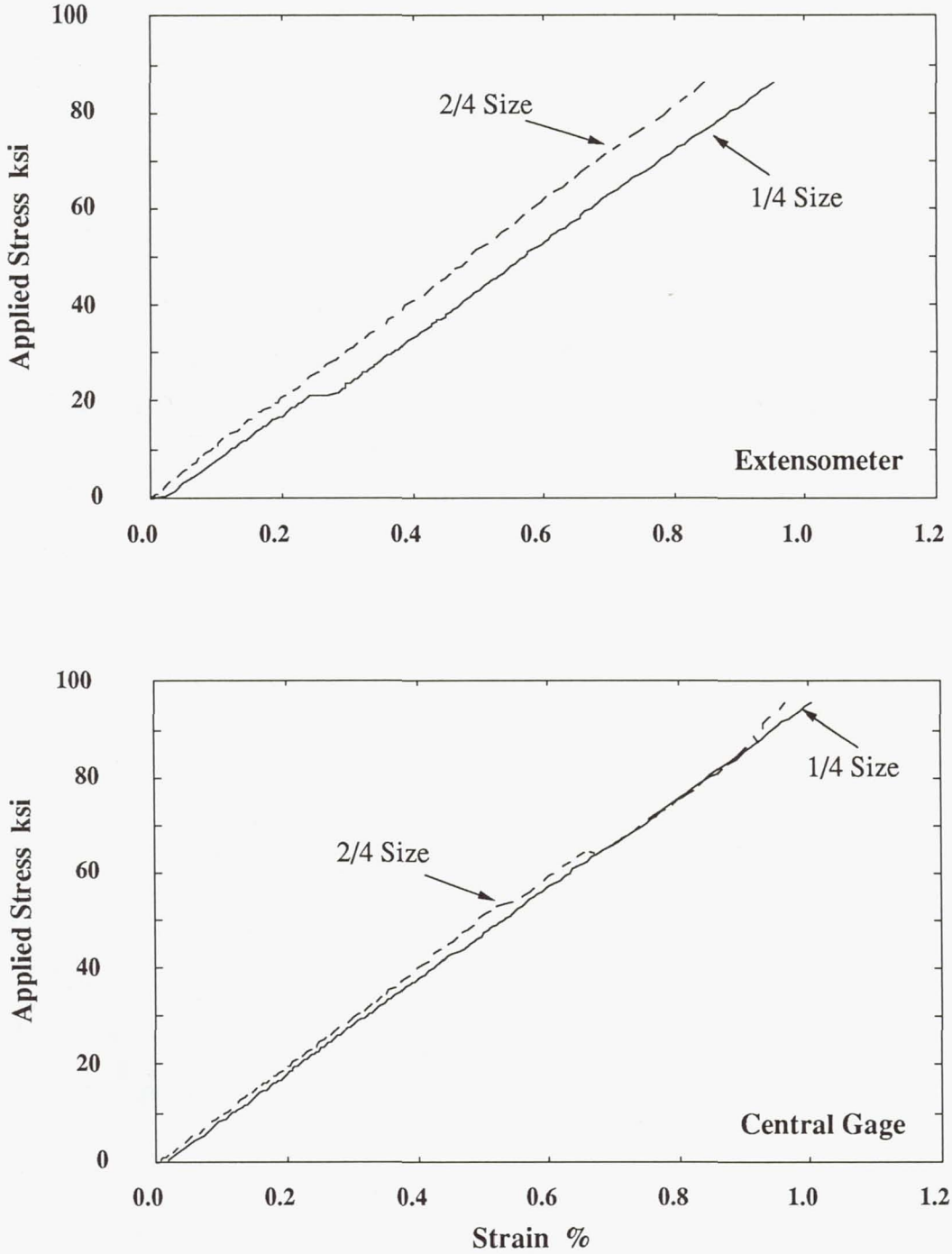

Fig.5 Stress/strain response for lay-up C. The strain was measured in two different ways (a) with an extensometer, and (b) with a centrally located strain gage.

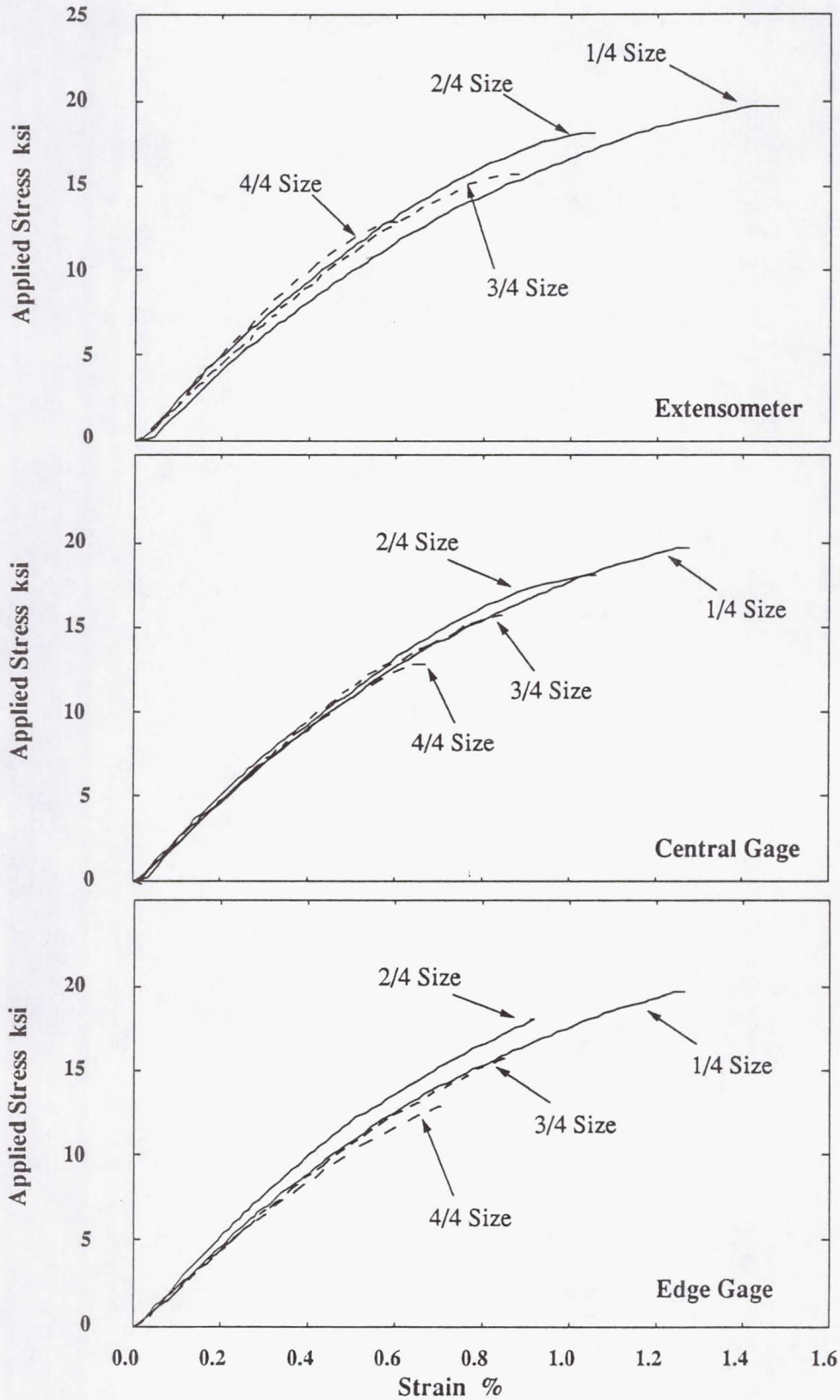

Fig.6 Stress/strain response for lay-up **D**. The strain was measured in three different ways: (a) with an extensometer, (b) with a series of centrally located strain gages, and (c) with one strain gage located close to the edge.

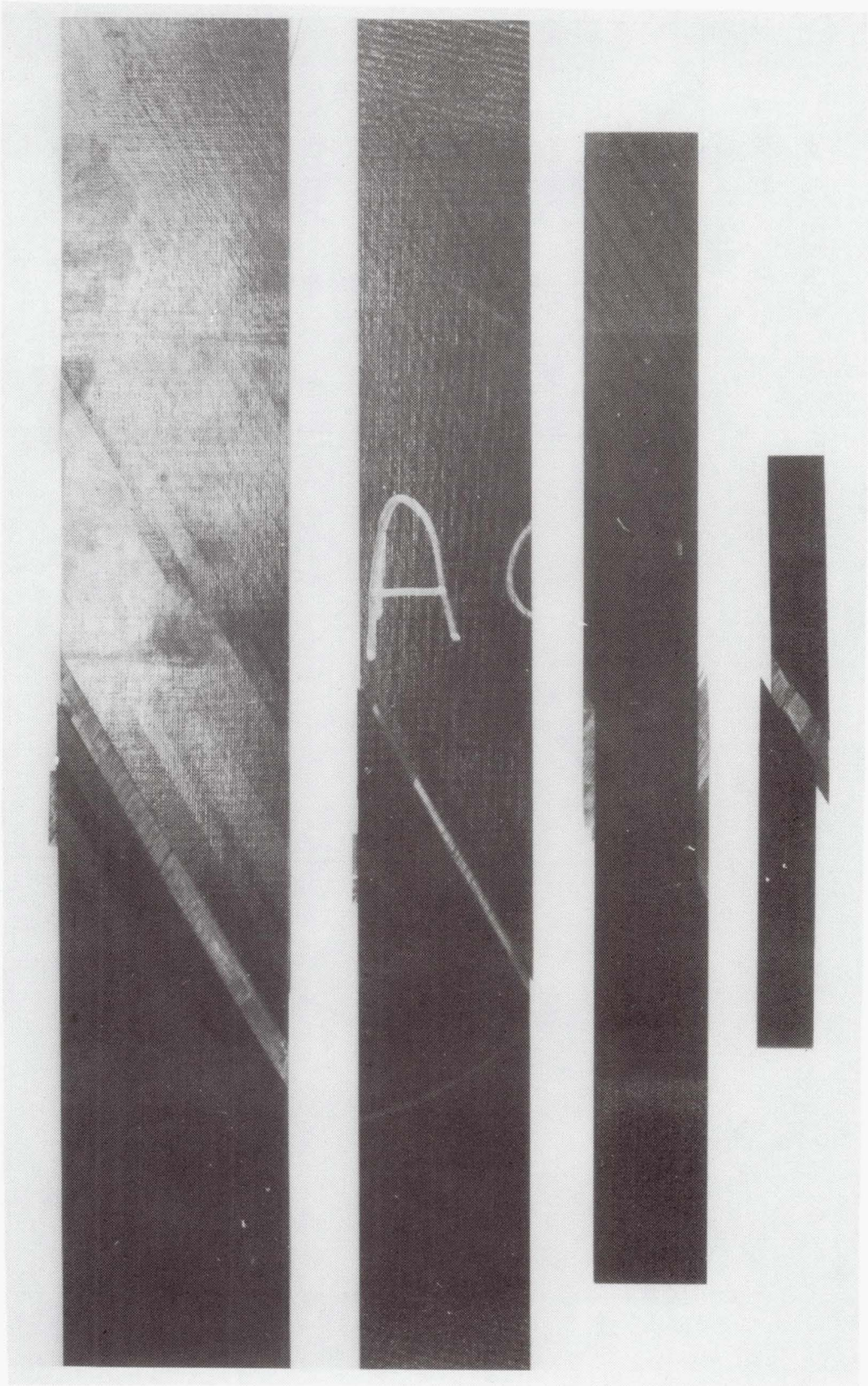

Fig.7 Typical modes of final failure in scaled specimens of lay-up **A**.

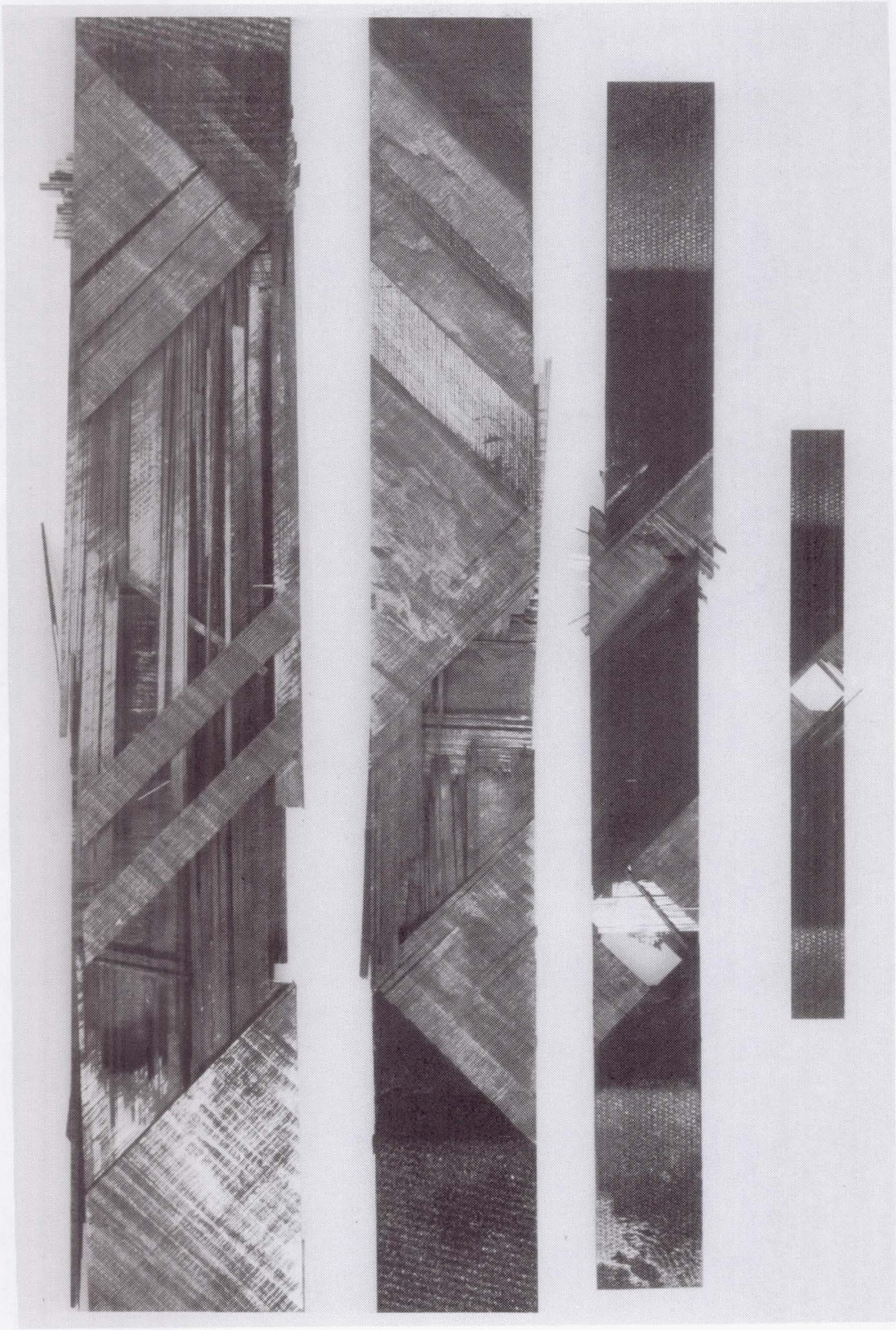

Fig.8 Typical modes of final failure in scaled specimens of lay-up **B**.

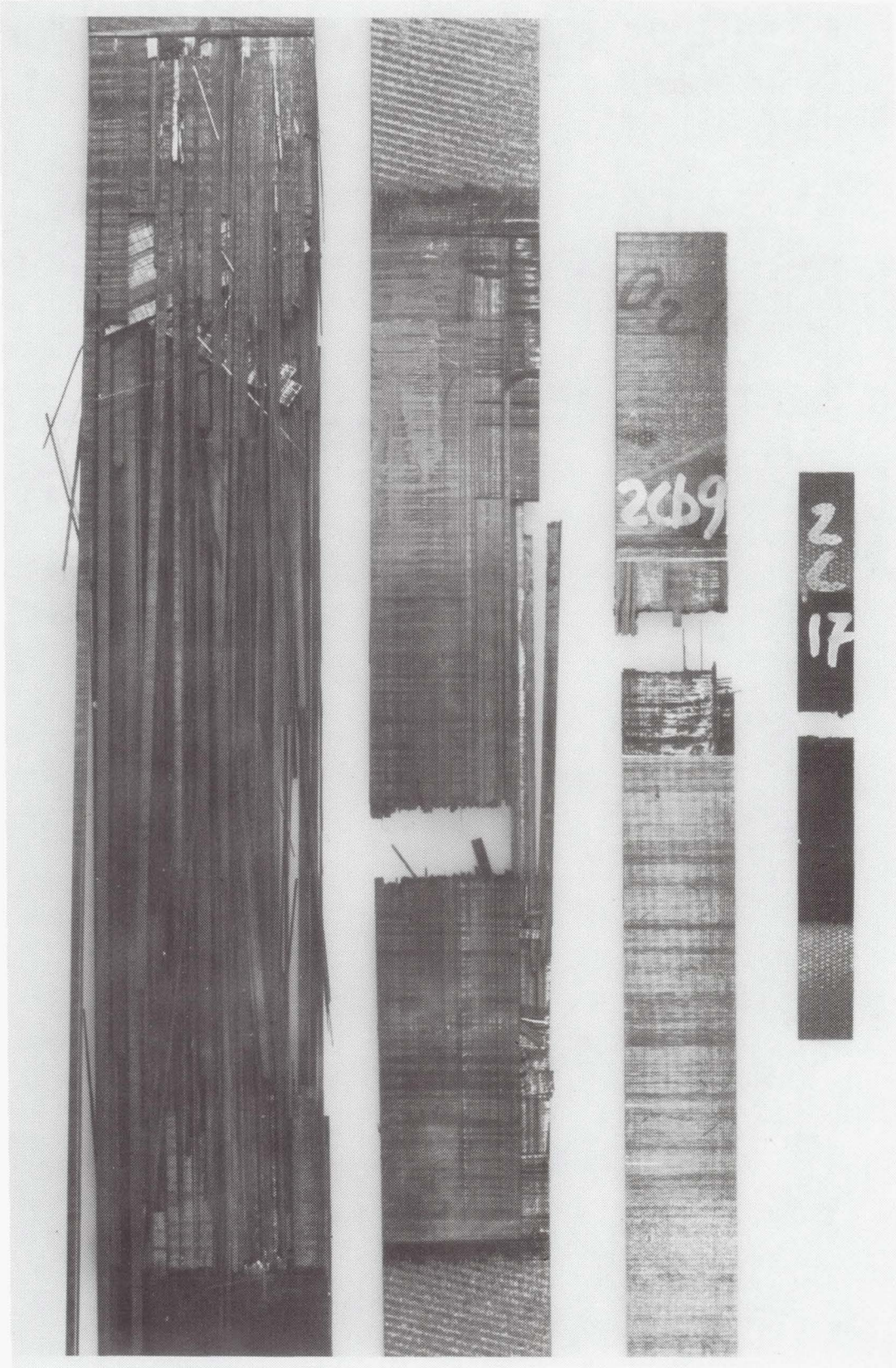

Fig.9 Typical modes of final failure in scaled specimens of lay-up **C**.

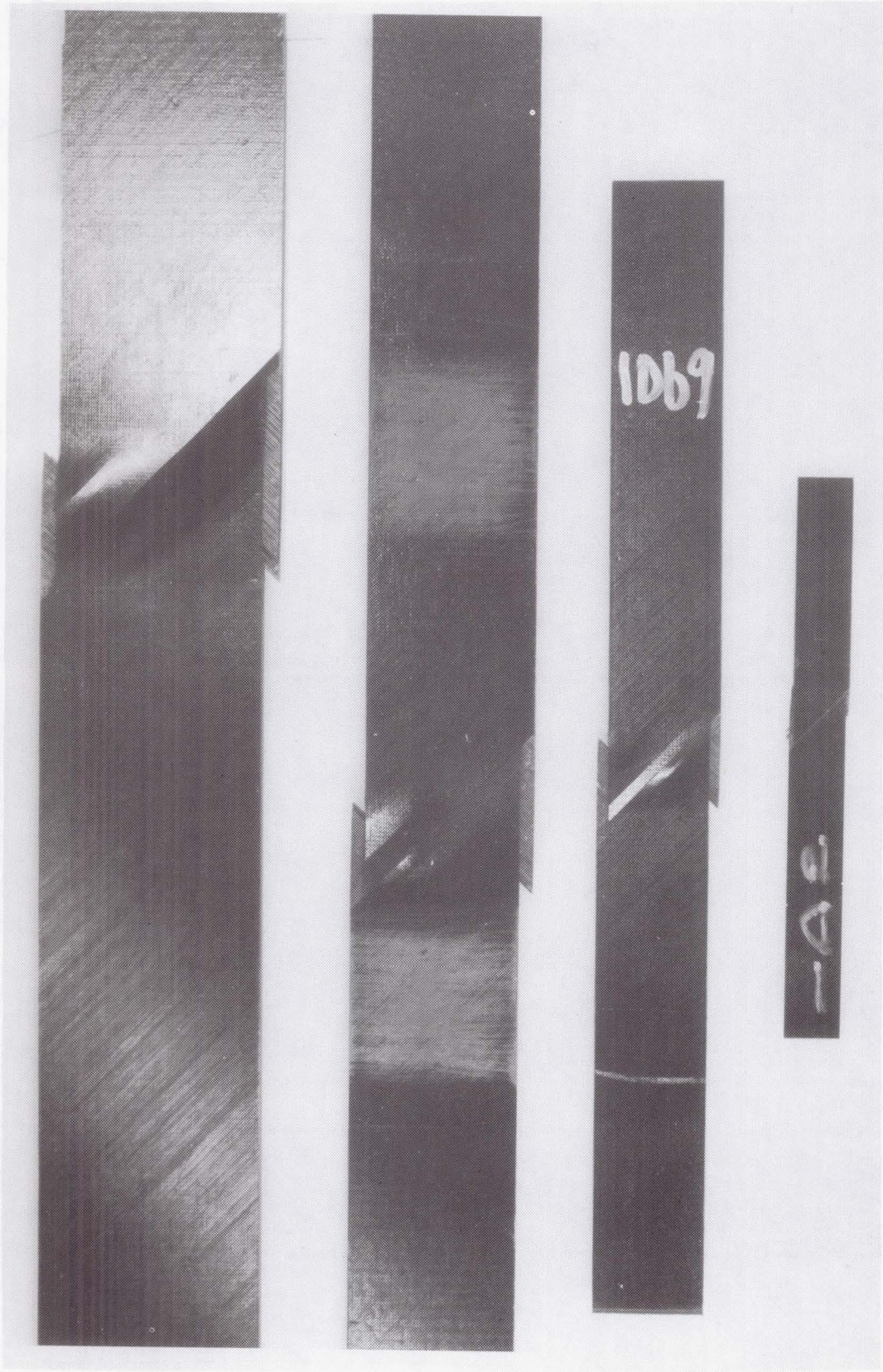

Fig.10 Typical modes of final failure in scaled specimens of lay-up **D**.

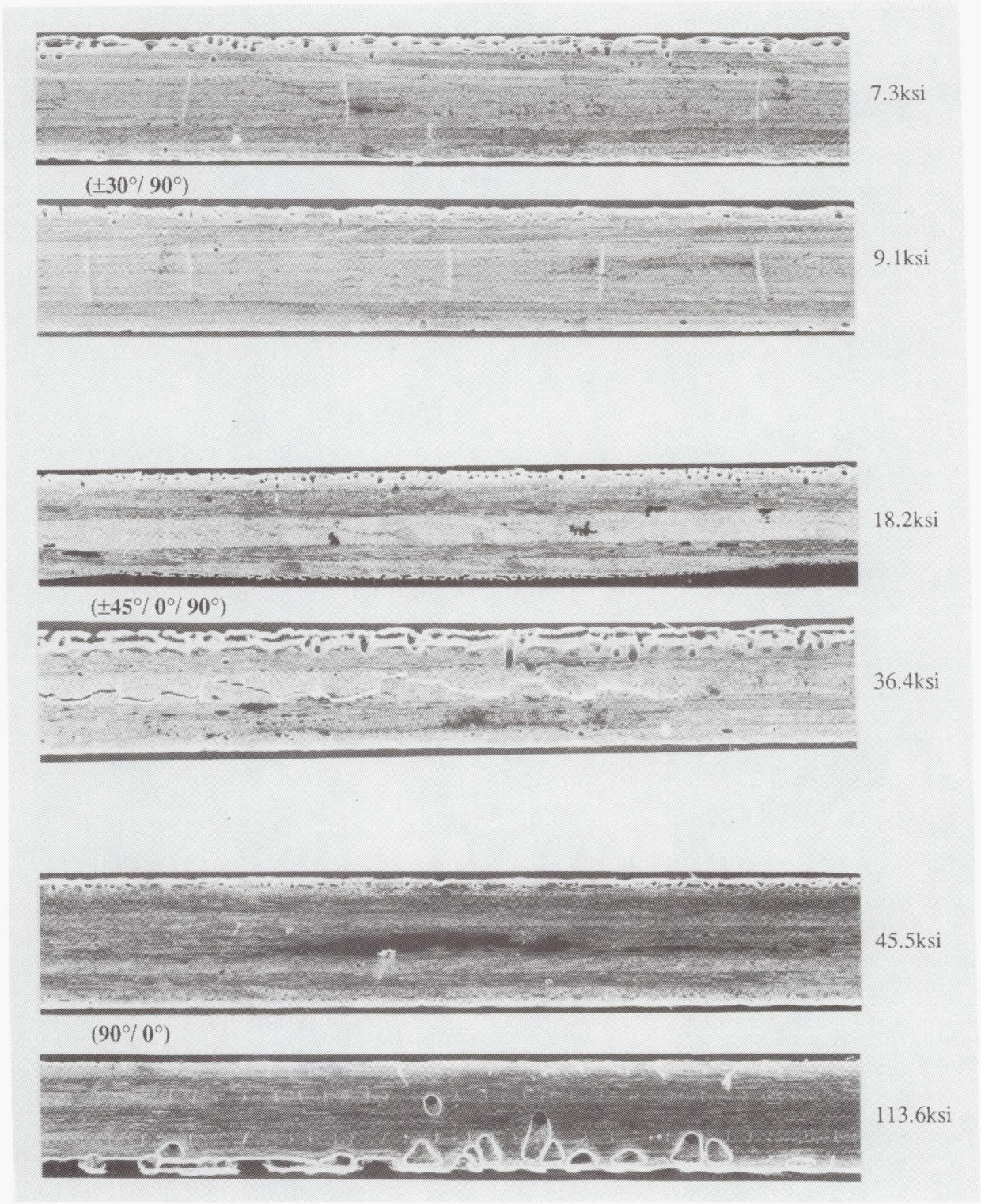

Fig.11 Typical edge replicas in three different lay-ups (**A**, **B** and **C**) for 1/4 size specimens. Progressive damage is shown after two load cases per lay-up.

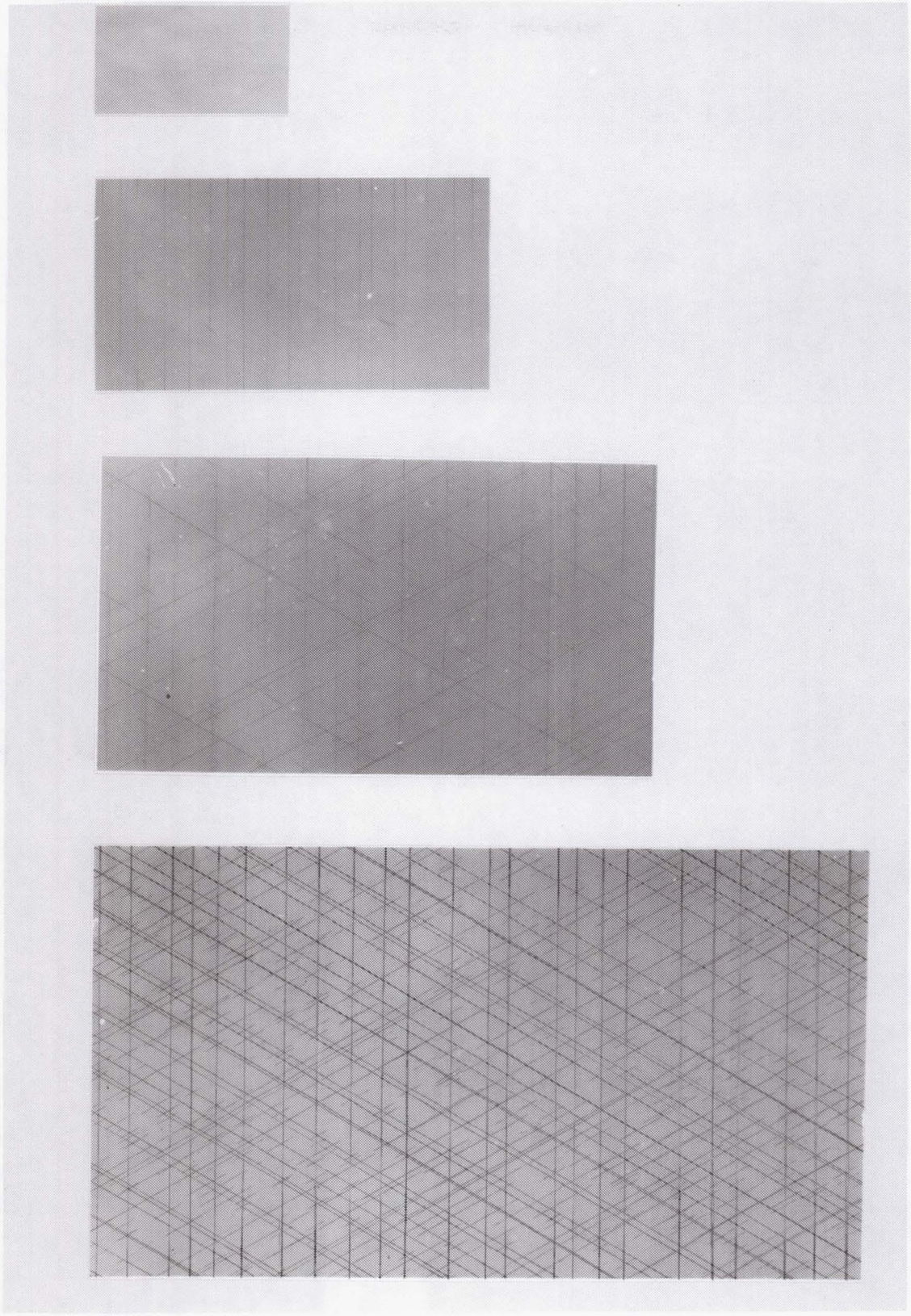

Fig.12 X-ray radiographs of virgin specimens of lay-up A.

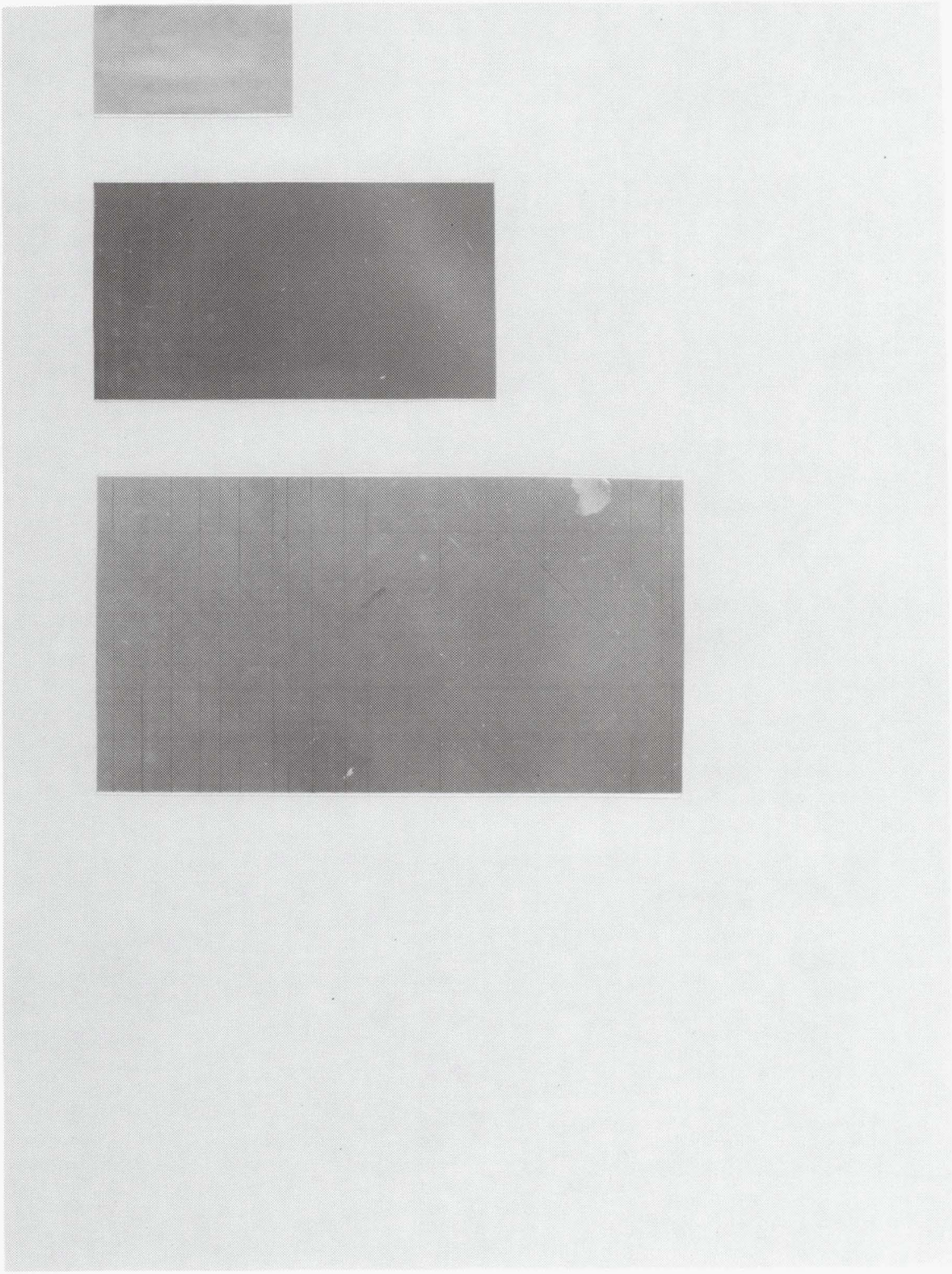

Fig.13 X-ray radiographs of virgin specimens of lay-up **B**. A virgin, full scale size specimen was not available at the time of test.

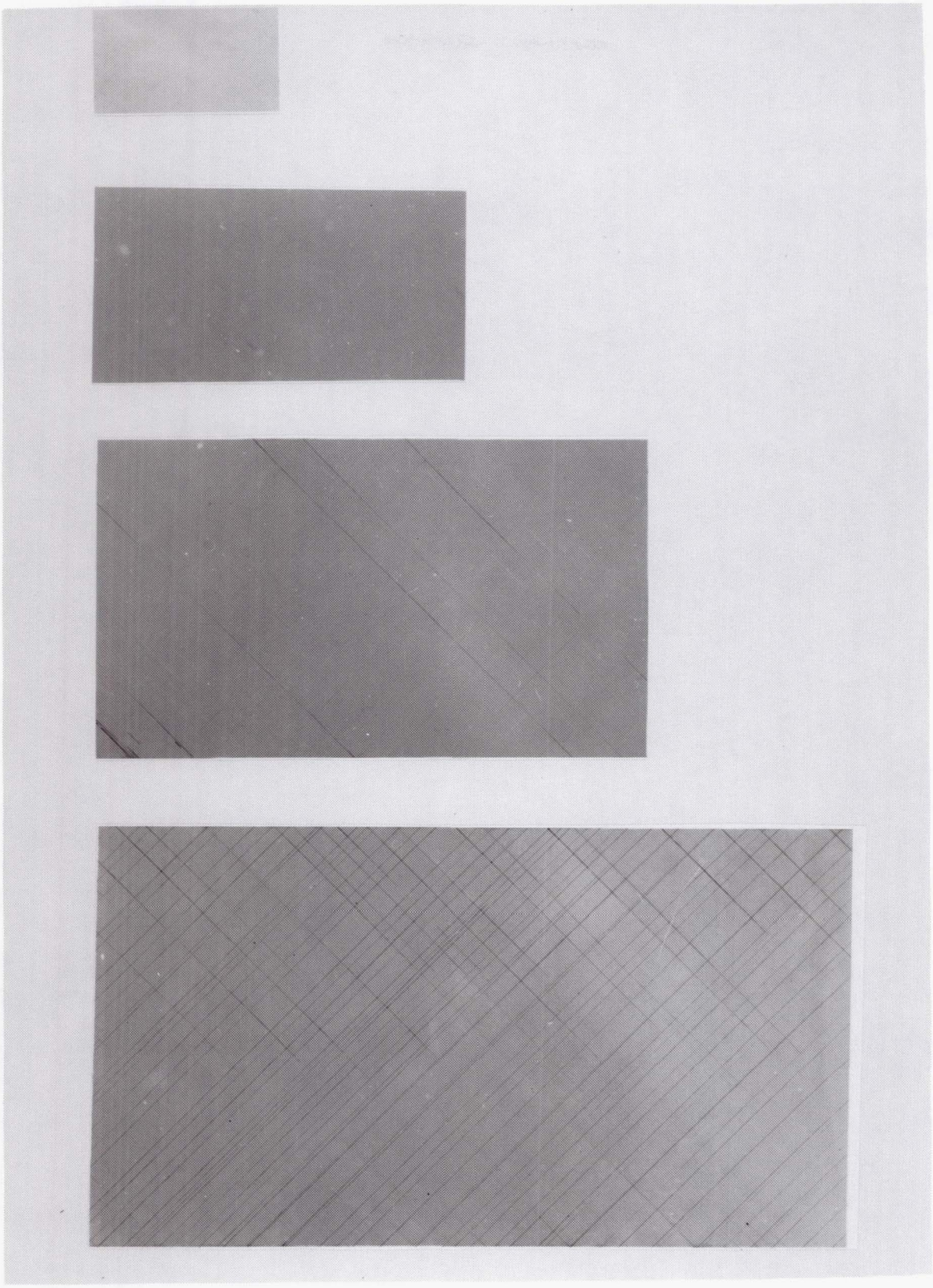

Fig.14 X-ray radiographs of virgin specimens of lay-up **D**.

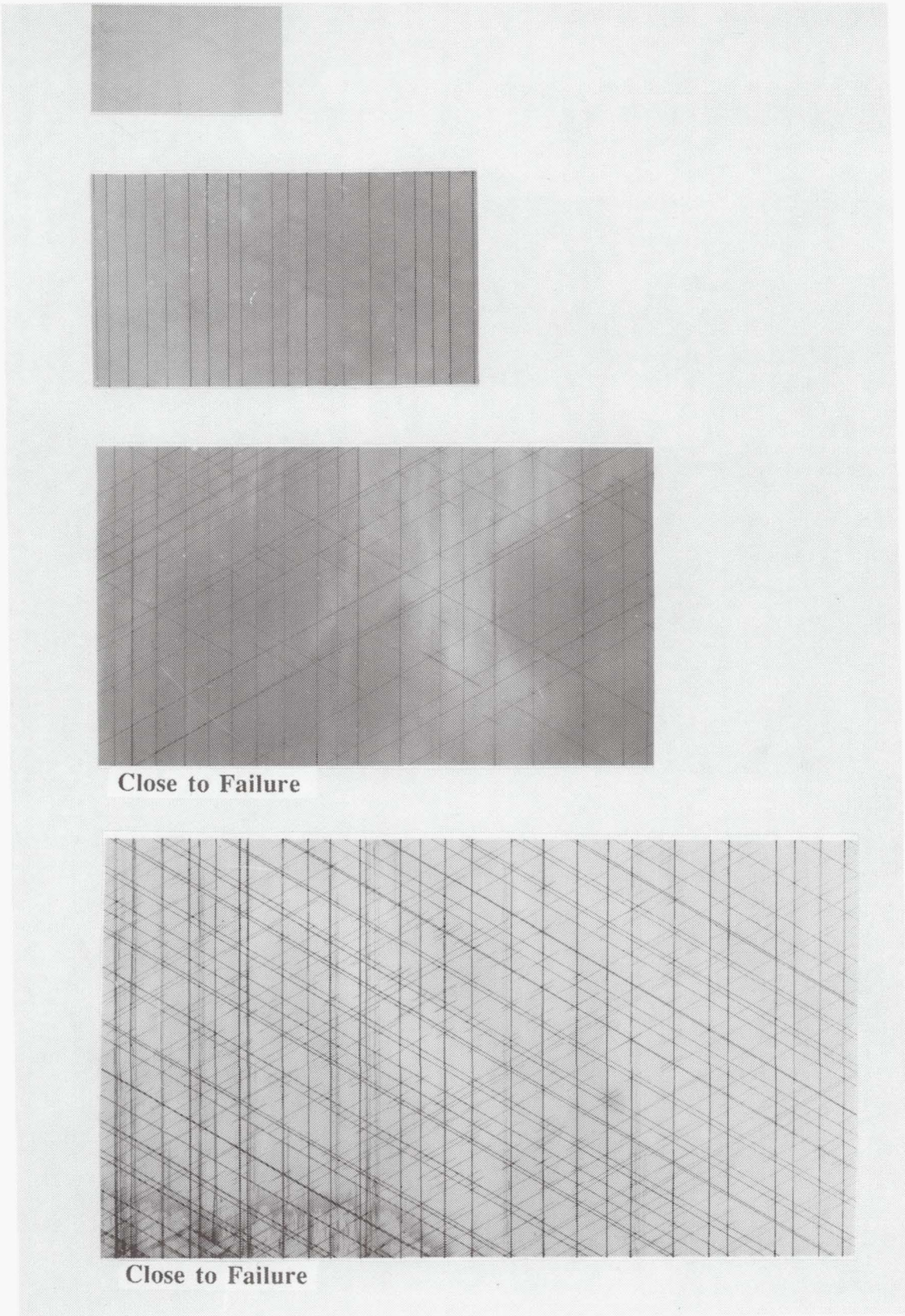

Fig.15 X-ray radiographs of pre-loaded specimens of lay-up **A**. Applied stress equal to **15** ksi.

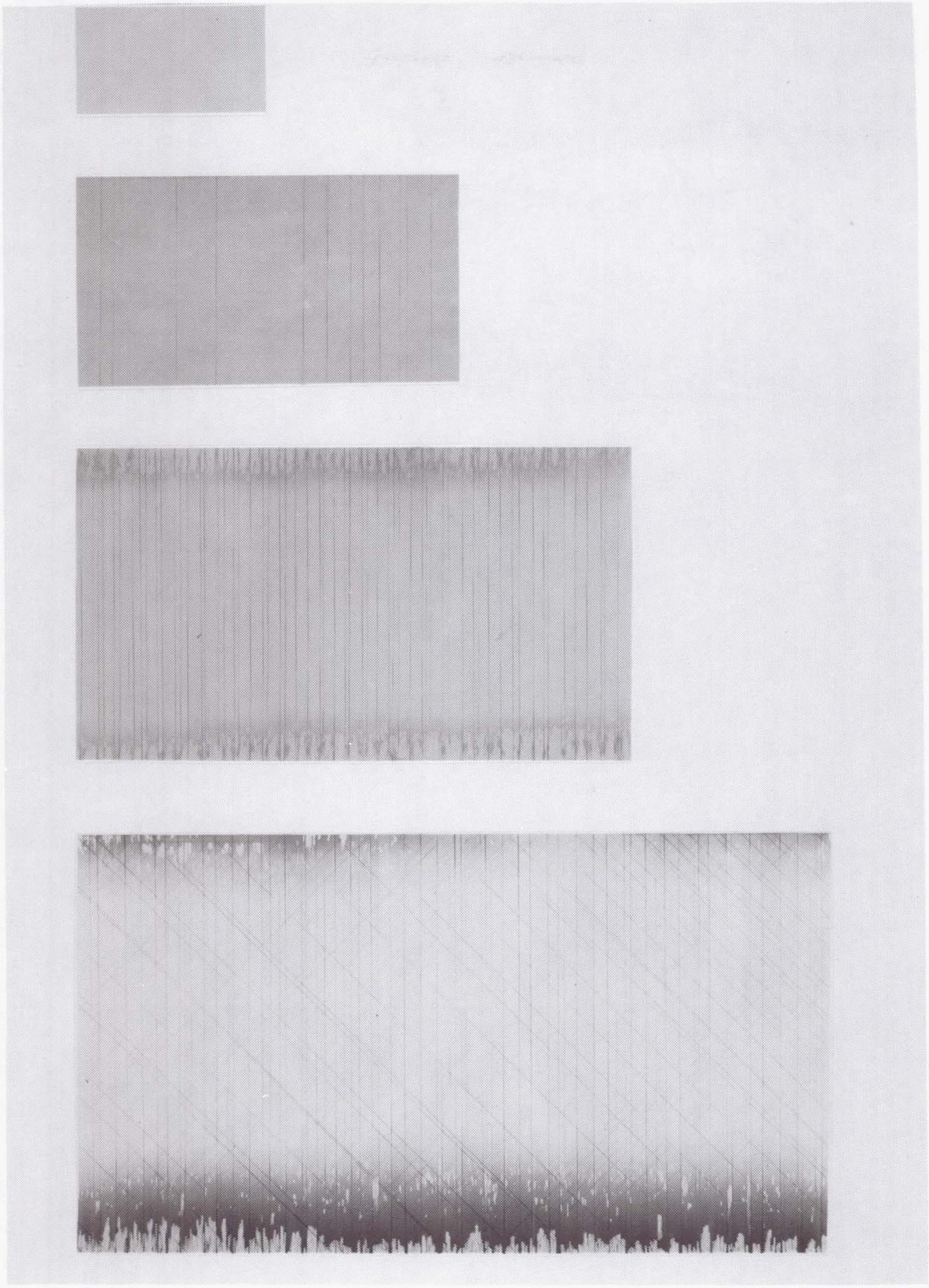

Fig.16 X-ray radiographs of pre-loaded specimens of lay-up **B**. Applied stress equal to **30** ksi.

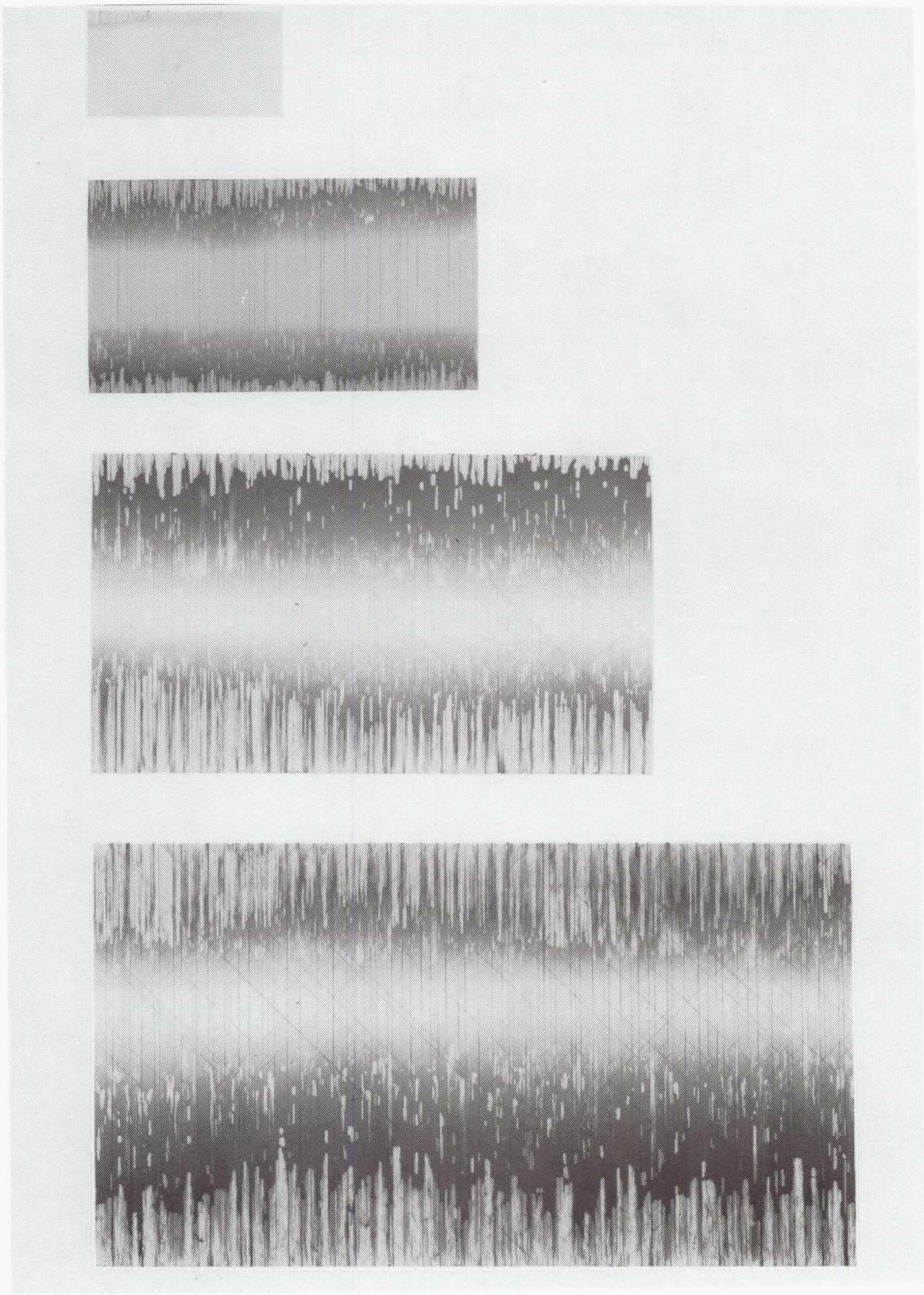

Fig.17 X-ray radiographs of pre-loaded specimens of lay-up **B**. Applied stress equal to **45** ksi.

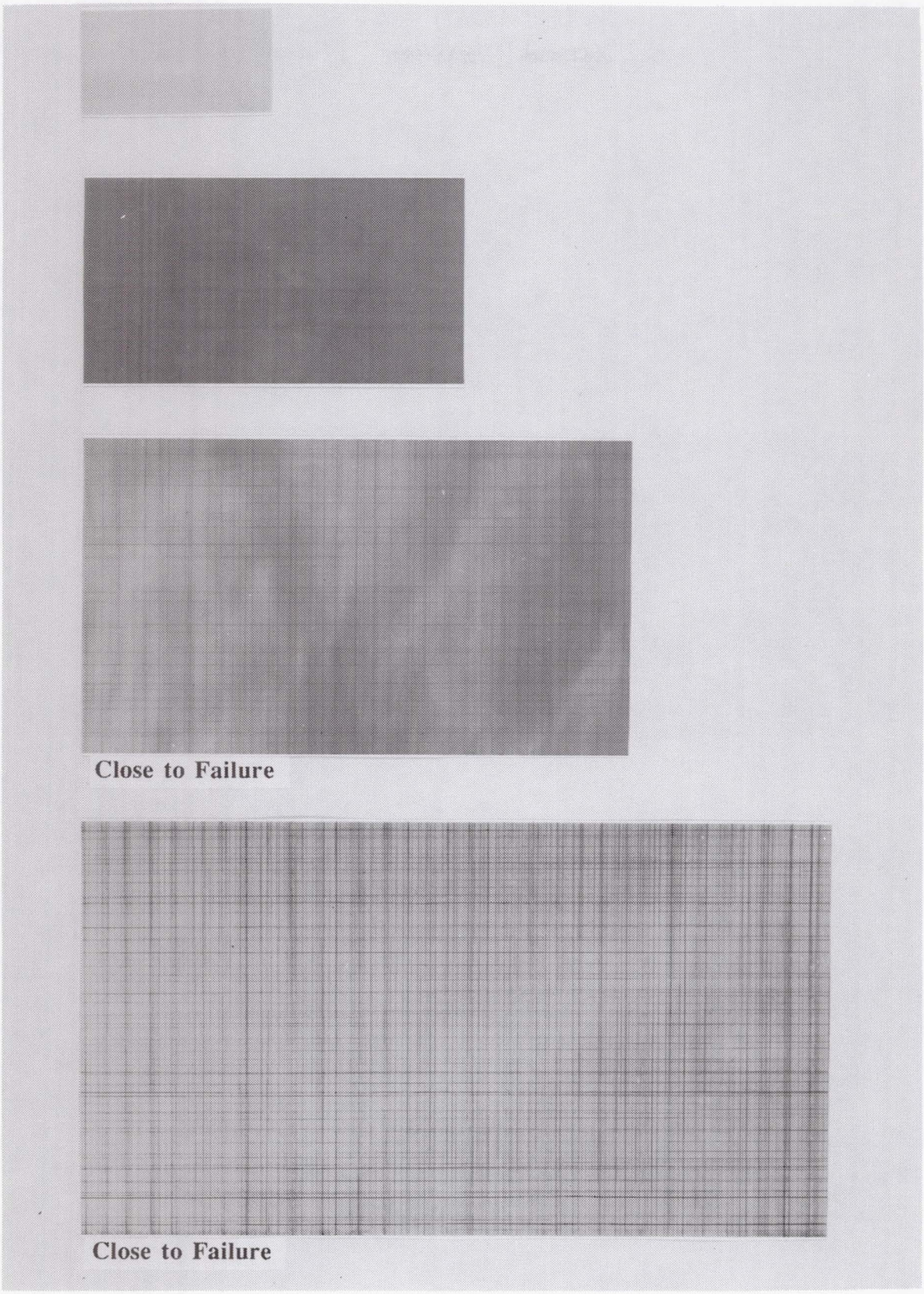

Fig.18 X-ray radiographs of pre-loaded specimens of lay-up **C**. Applied stress equal to **69** ksi.

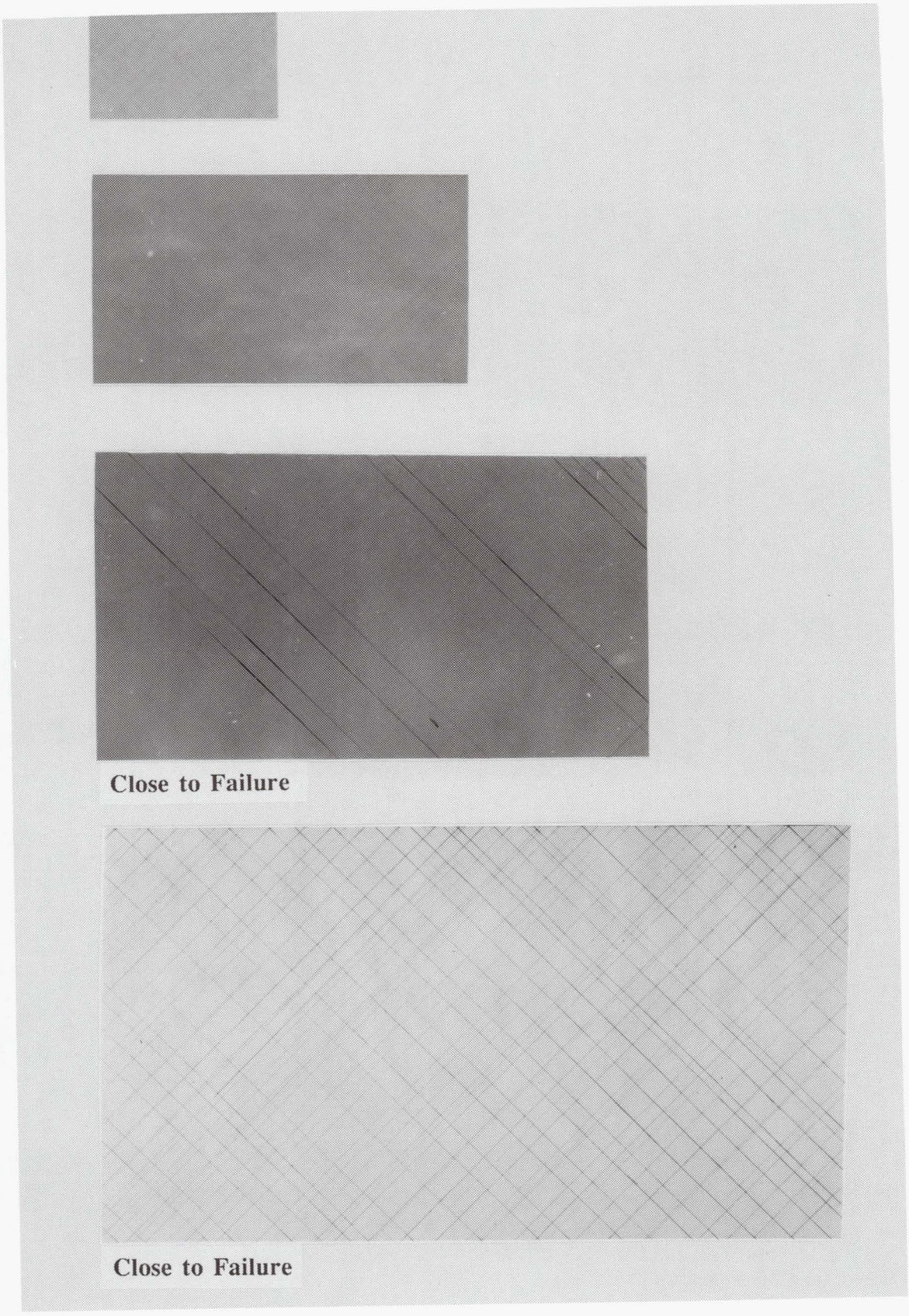

Fig.19 X-ray radiographs of pre-loaded specimens of lay-up **D**. Applied stress equal to **12** ksi.

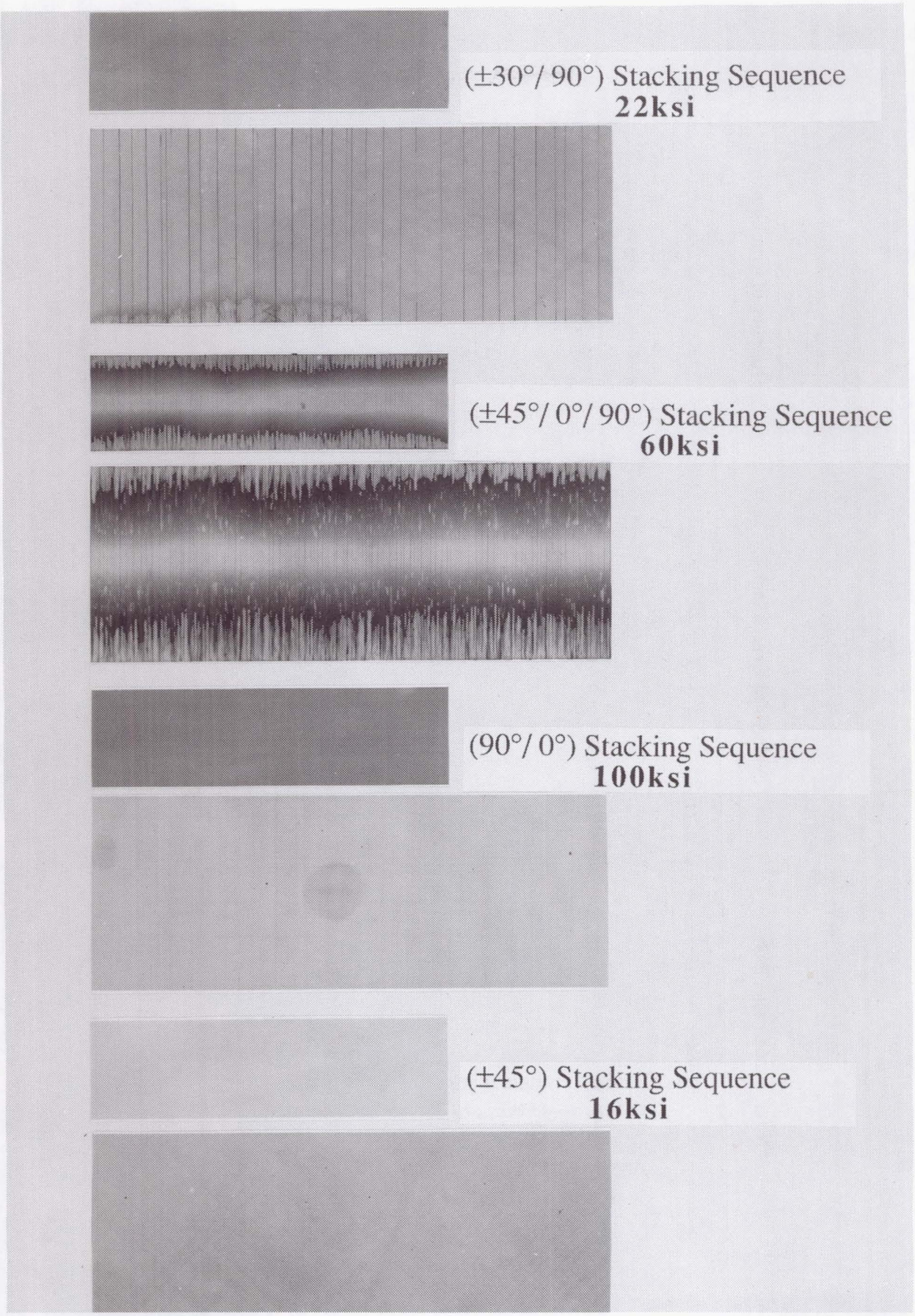

Fig.20 X-ray radiographs of pre-loaded 1/4 and 2/4 size specimens, for all four lay-ups. All specimens were loaded to near failure.

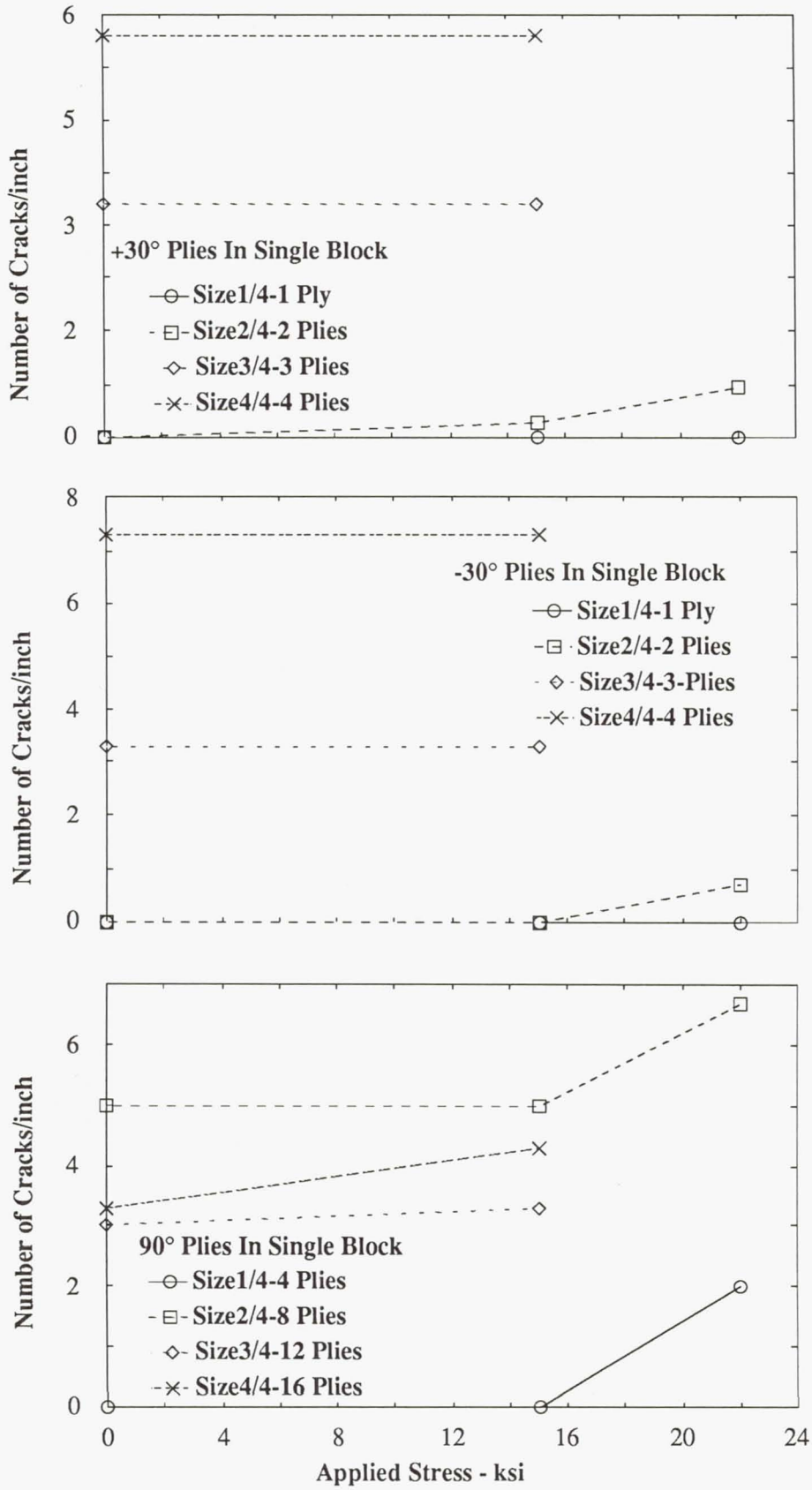

Fig. 21 Crack density versus applied load in individual groups of plies in lay-up **A**.

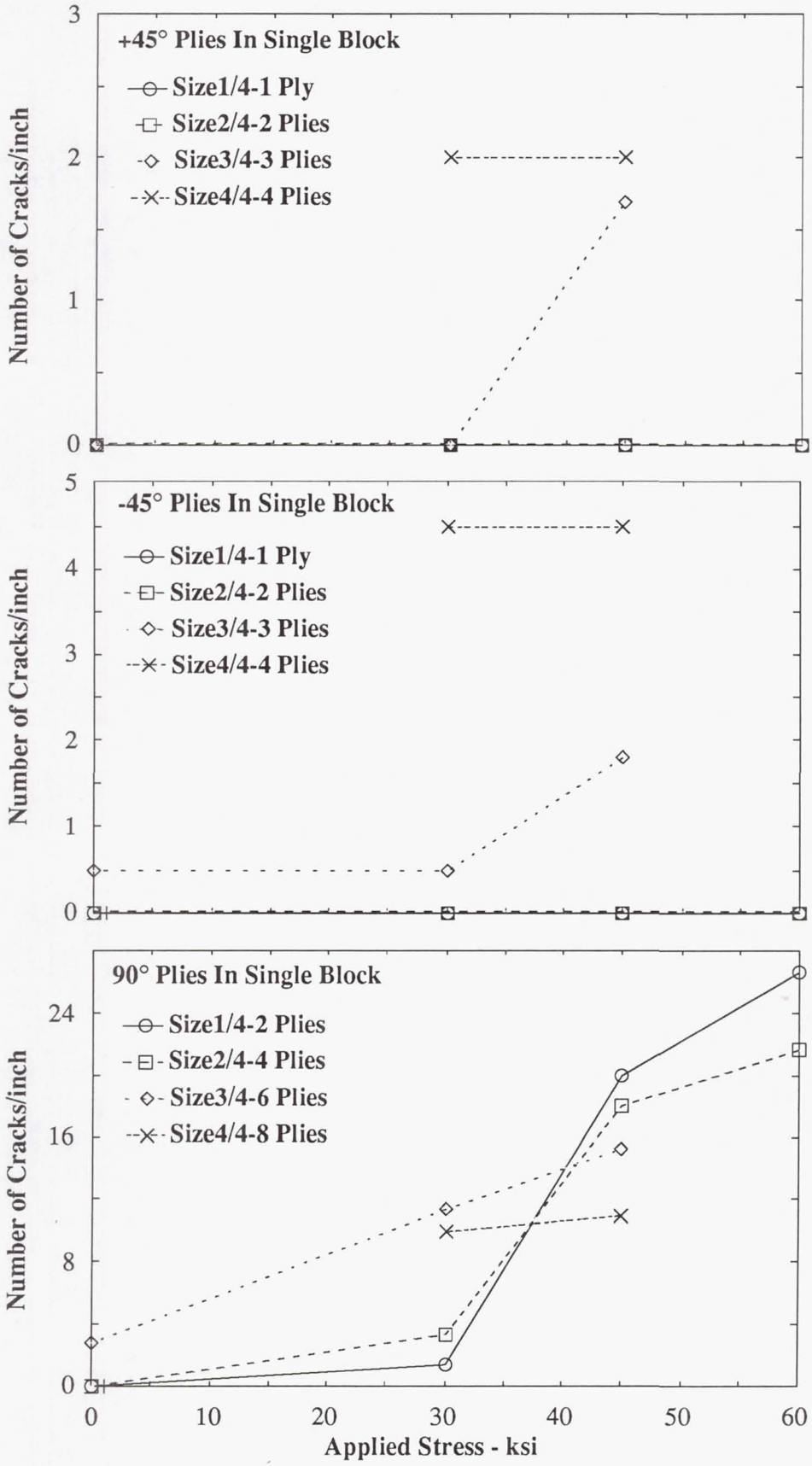

Fig. 22 Crack density versus applied load in individual groups of plies in lay-up **B.**

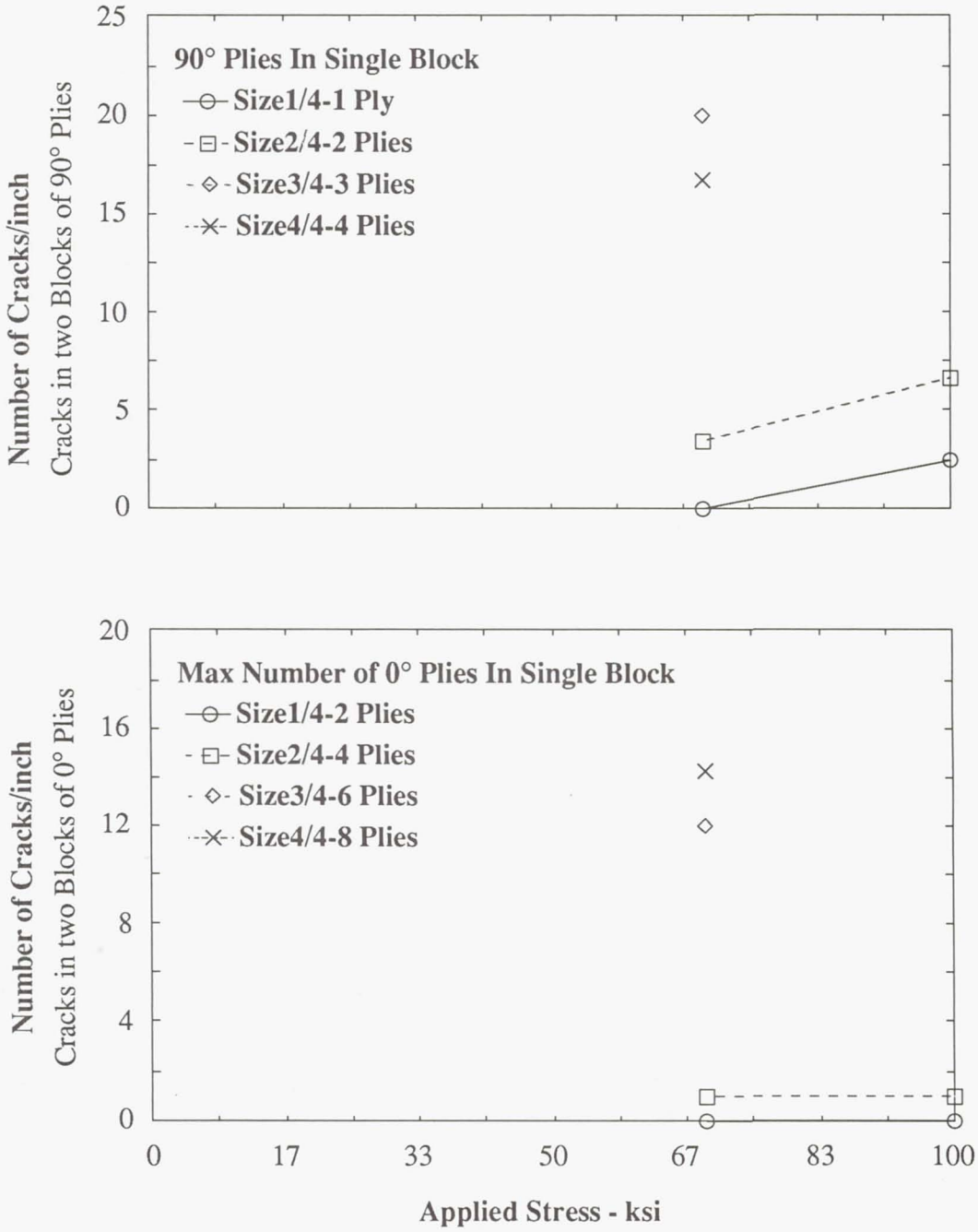

Fig. 23 Crack density versus applied load in individual groups of plies in lay-up **C.**

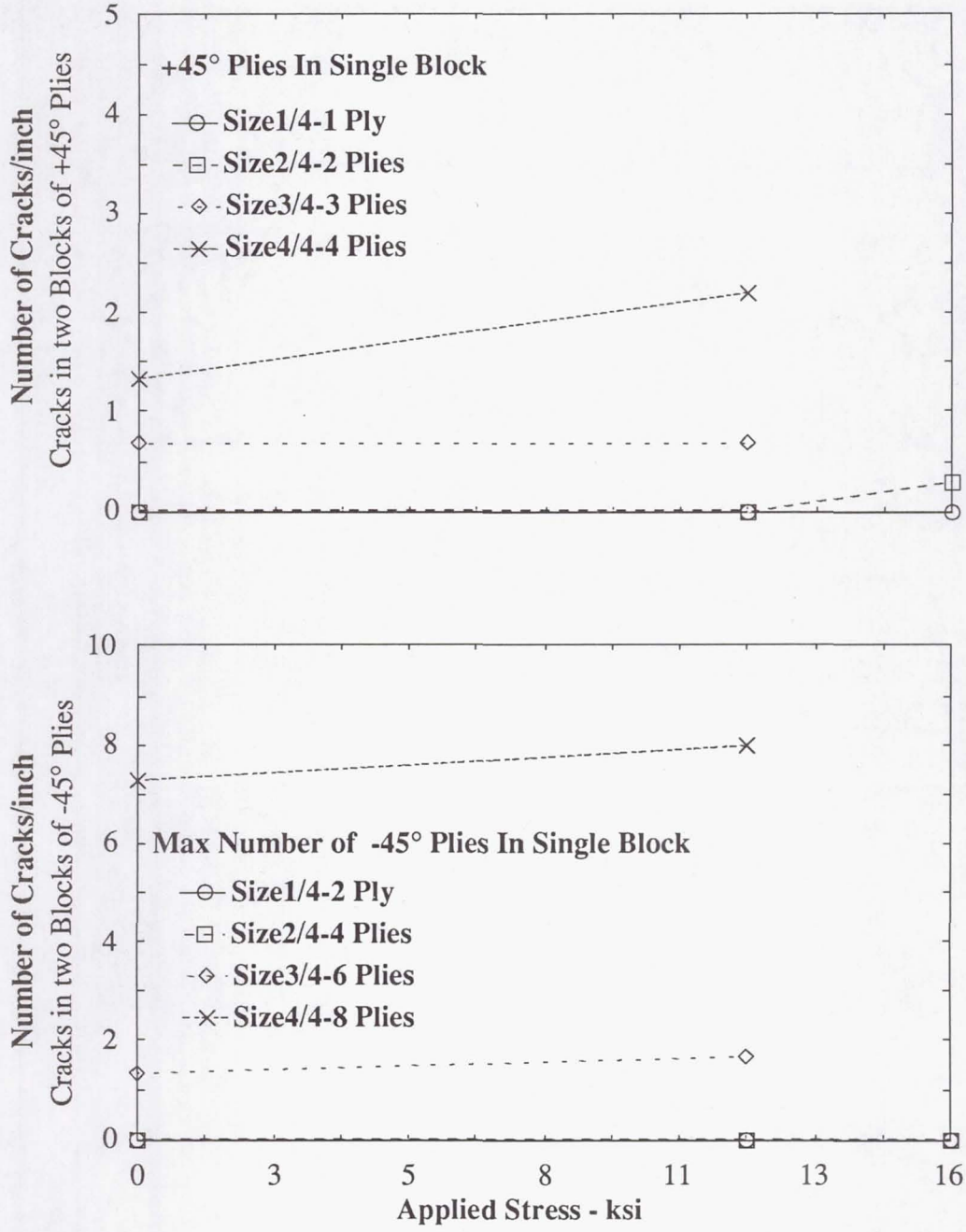

Fig. 24 Crack density versus applied load in individual groups of plies in lay-up **D.**

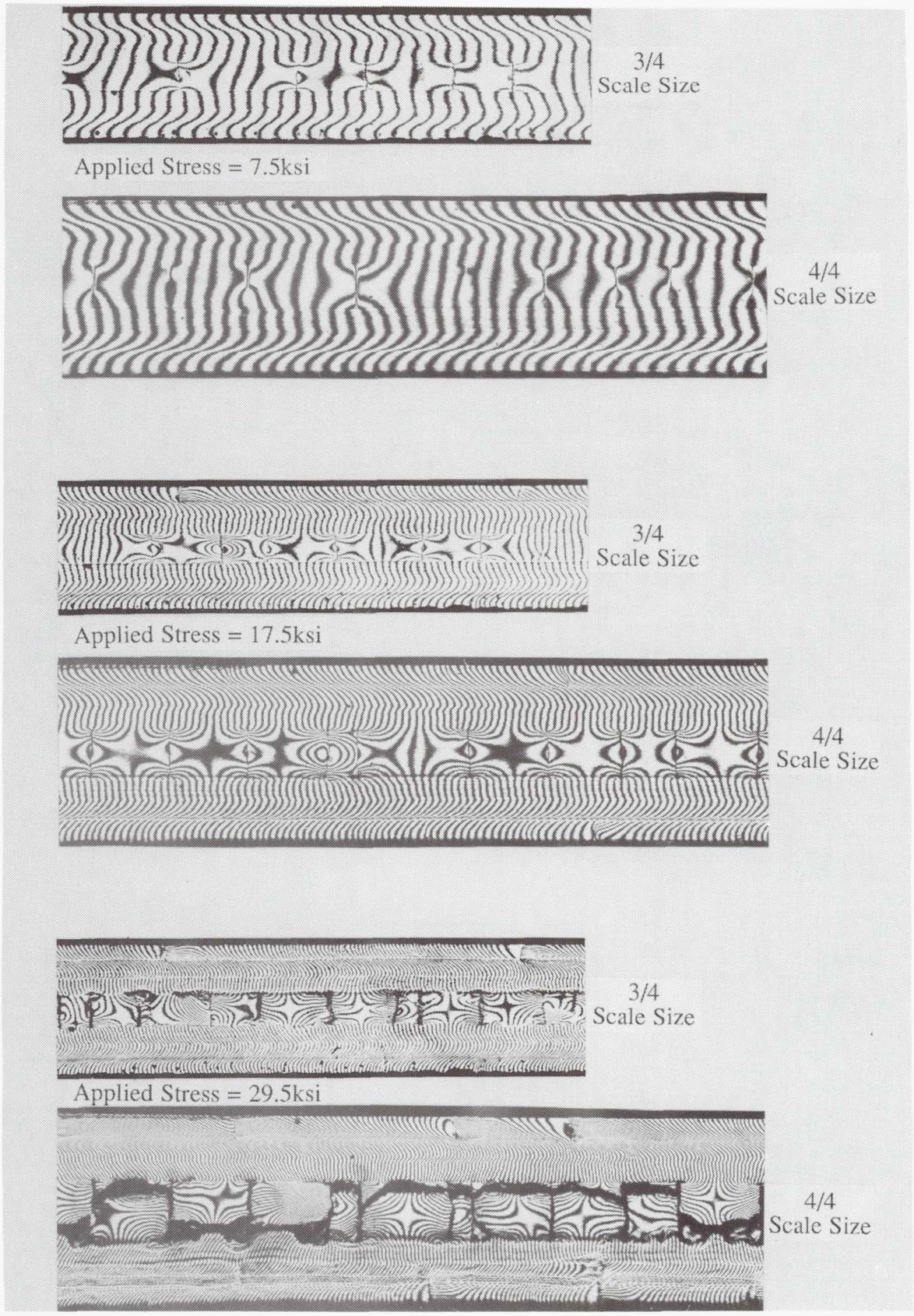

Fig.25 Free edge x-displacement distribution, for lay-up **B** $(\pm 45°_n/0°_n/90°_n)_s$, by moire' interferometry. n=3 and 4 for the 3/4 and 4/4 scale size specimens respectively and the x-displacement is along the loading direction.

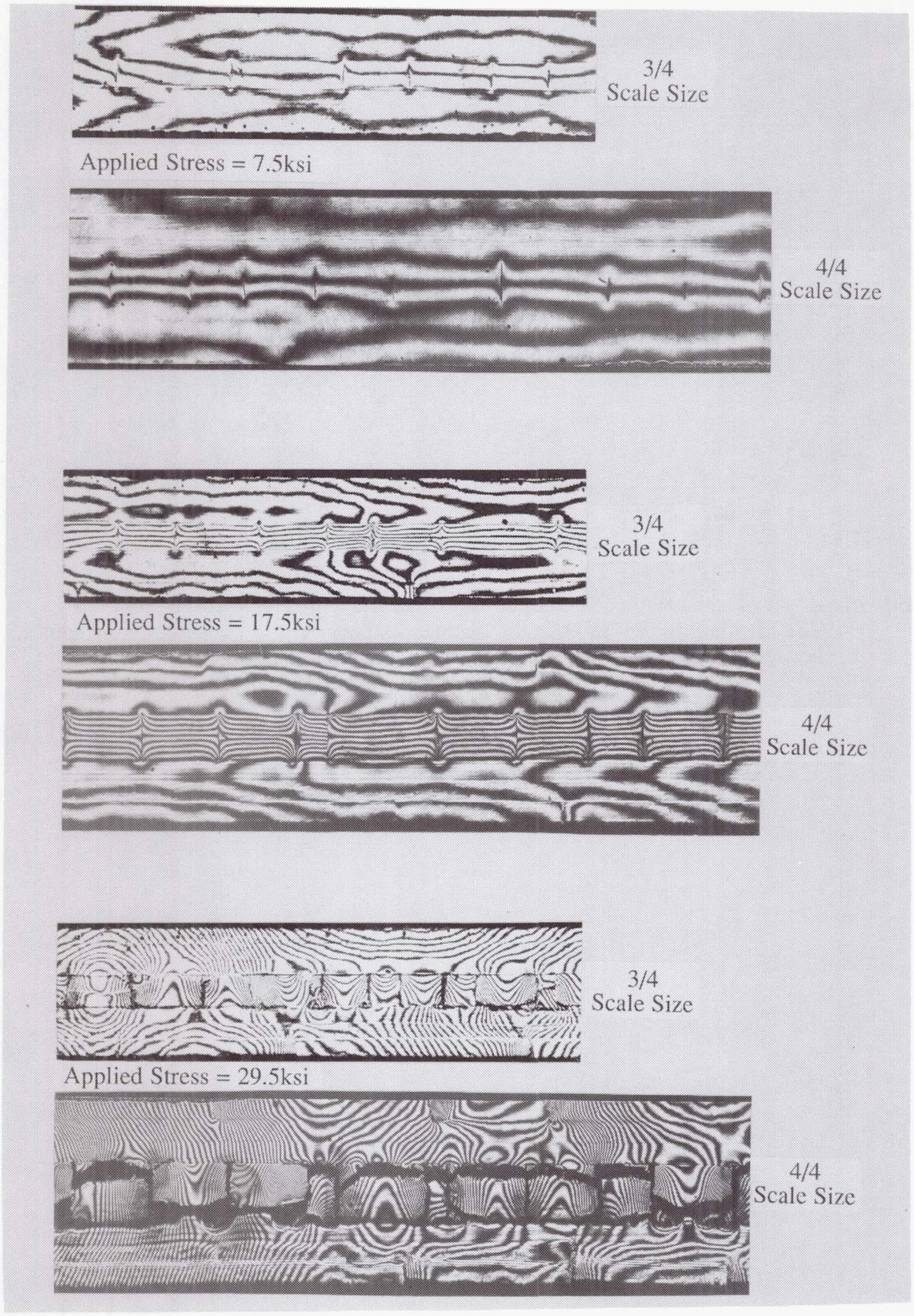

Fig.26 Free edge z-displacement distribution, for lay-up **B** $(\pm 45°_n/0°_n/90°_n)_s$, by moire' interferometry. n=3 and 4 for the 3/4 and 4/4 scale size specimens respectively and the z-displacement is along the specimen thickness direction.

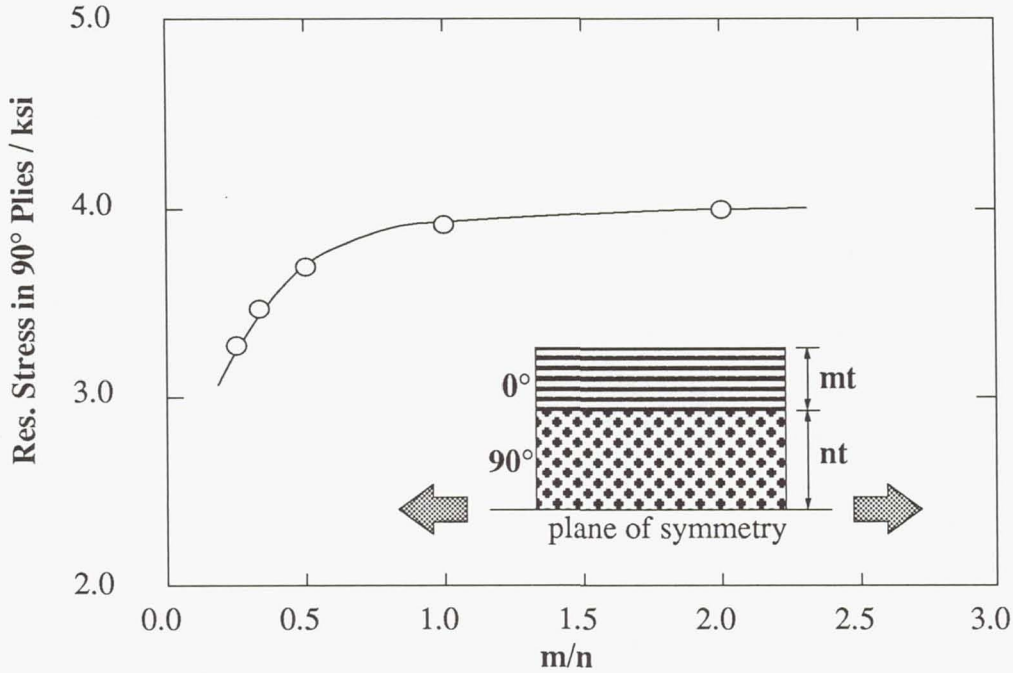

Fig. 27 Residual stress in the 90° plies of a (0°m/90°n)s laminate versus the m/n ratio. The calculations are based on the lamination theory with a temperature difference, between the stress free state and the room temperature, of 180 °F.

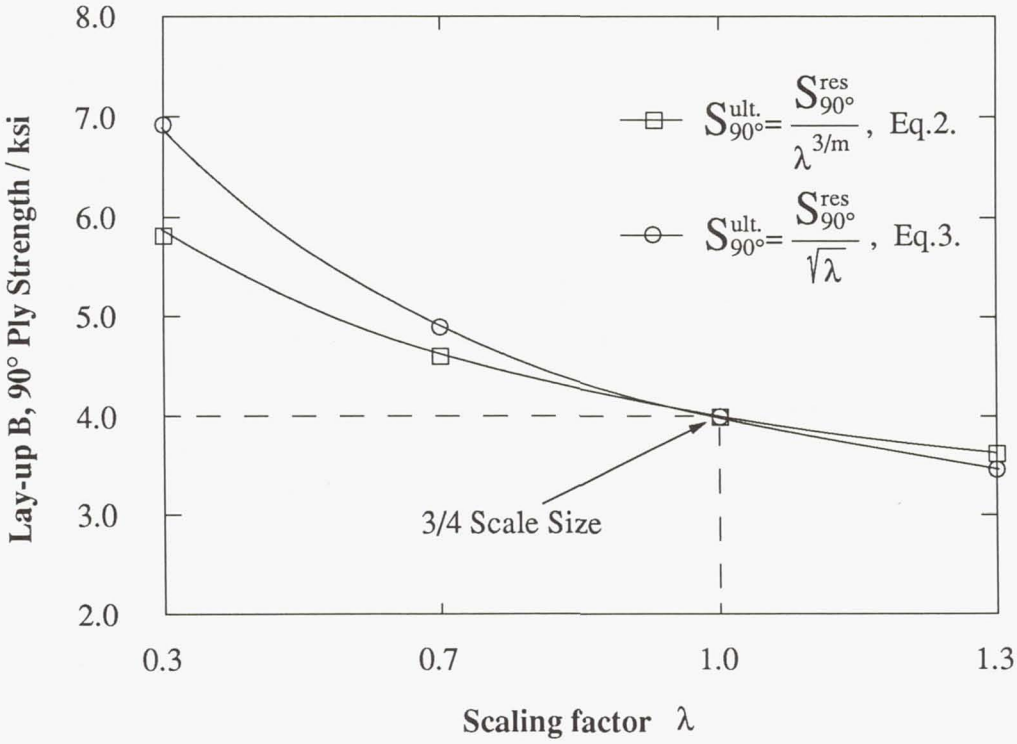

Fig. 28 Strength versus ply thickness for the 90° plies of lay-up **B**, (±45°n/0°n/90°n)s, based on strength predictions by Eqs. 2 and 3.

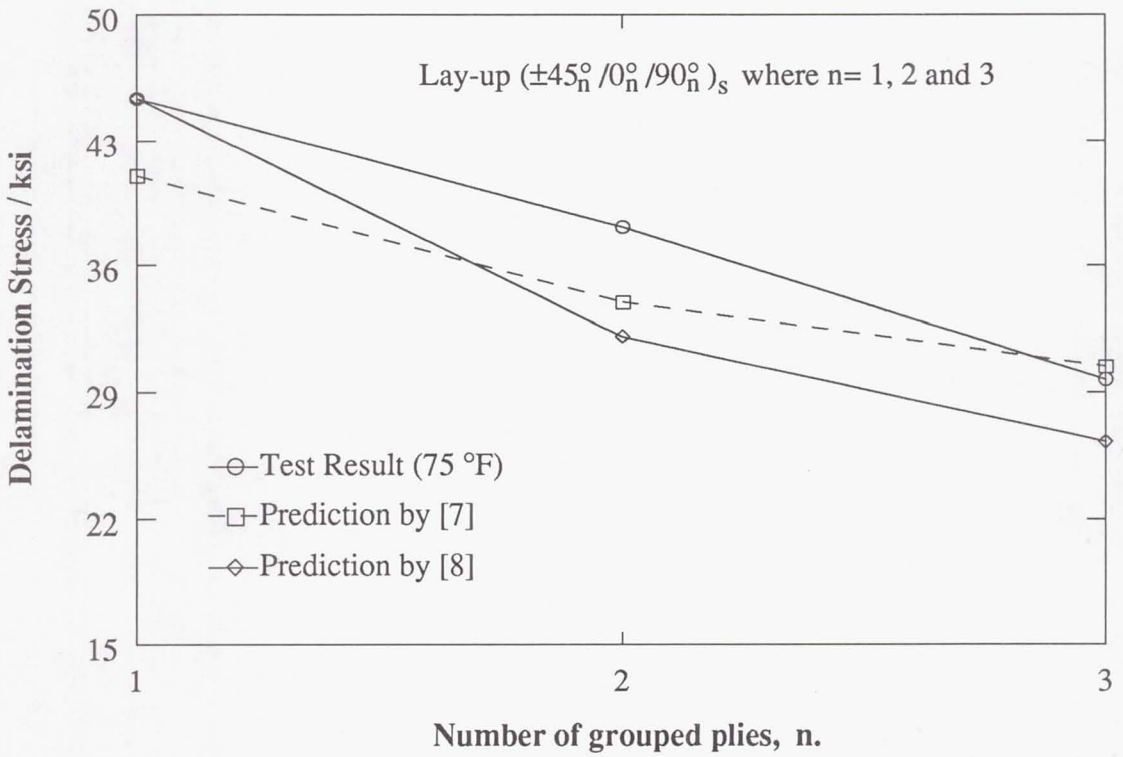

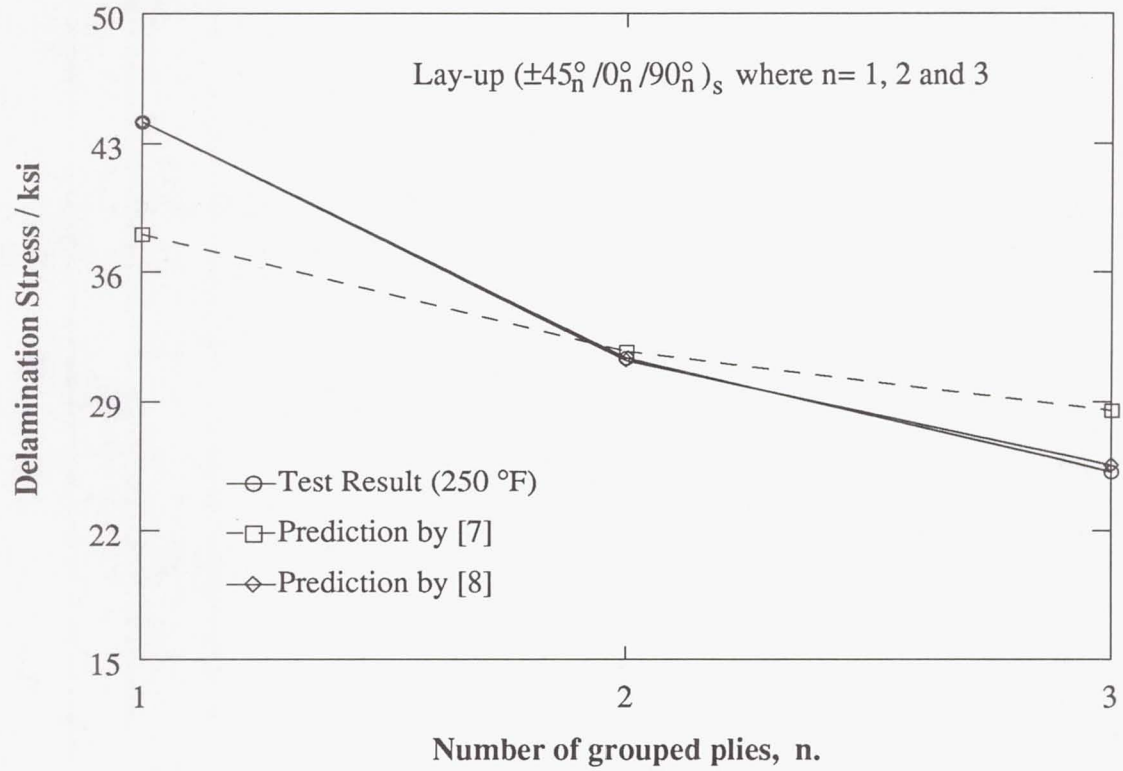

Fig. 29 Delamination stress versus n for a quasi-isotropic lay-up (±45°n/0°n/90°n)s. A comparison between theory by [7], experiment by [7], and Eq.3 by [8].

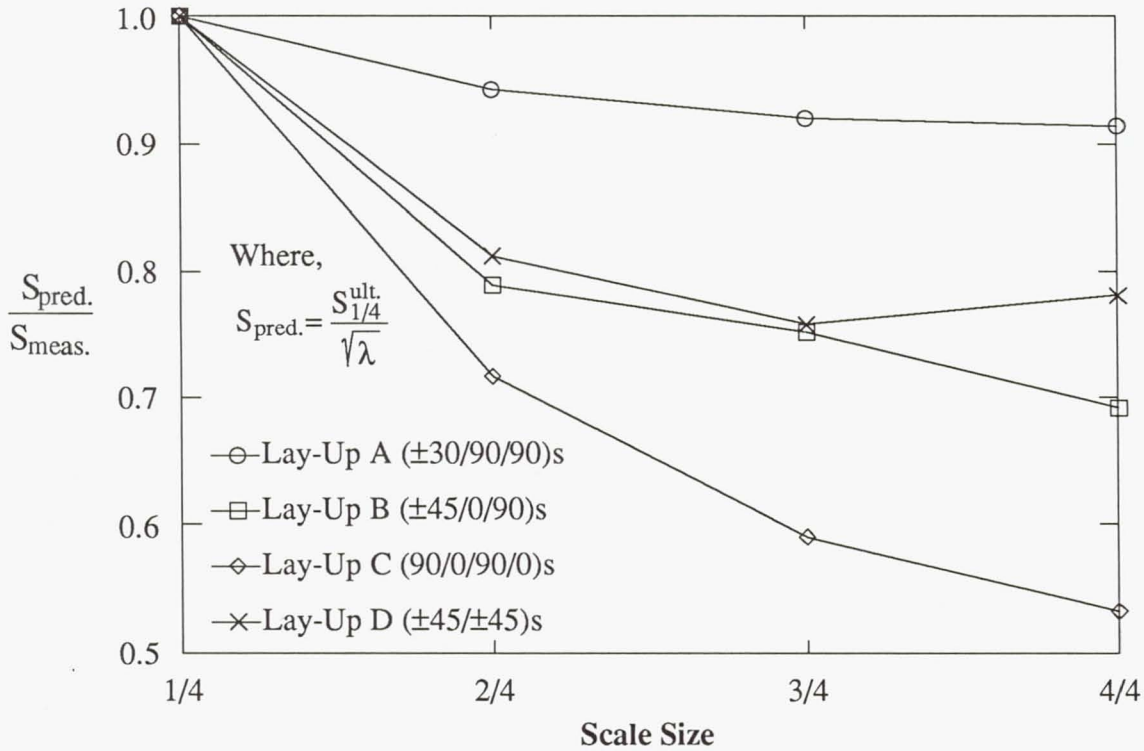

Fig. 30 Correlation between the fracture mechanics based model, Eq.3, and the experimentally obtained strengths for lay-ups **A**, **B**, **C**, and **D**.

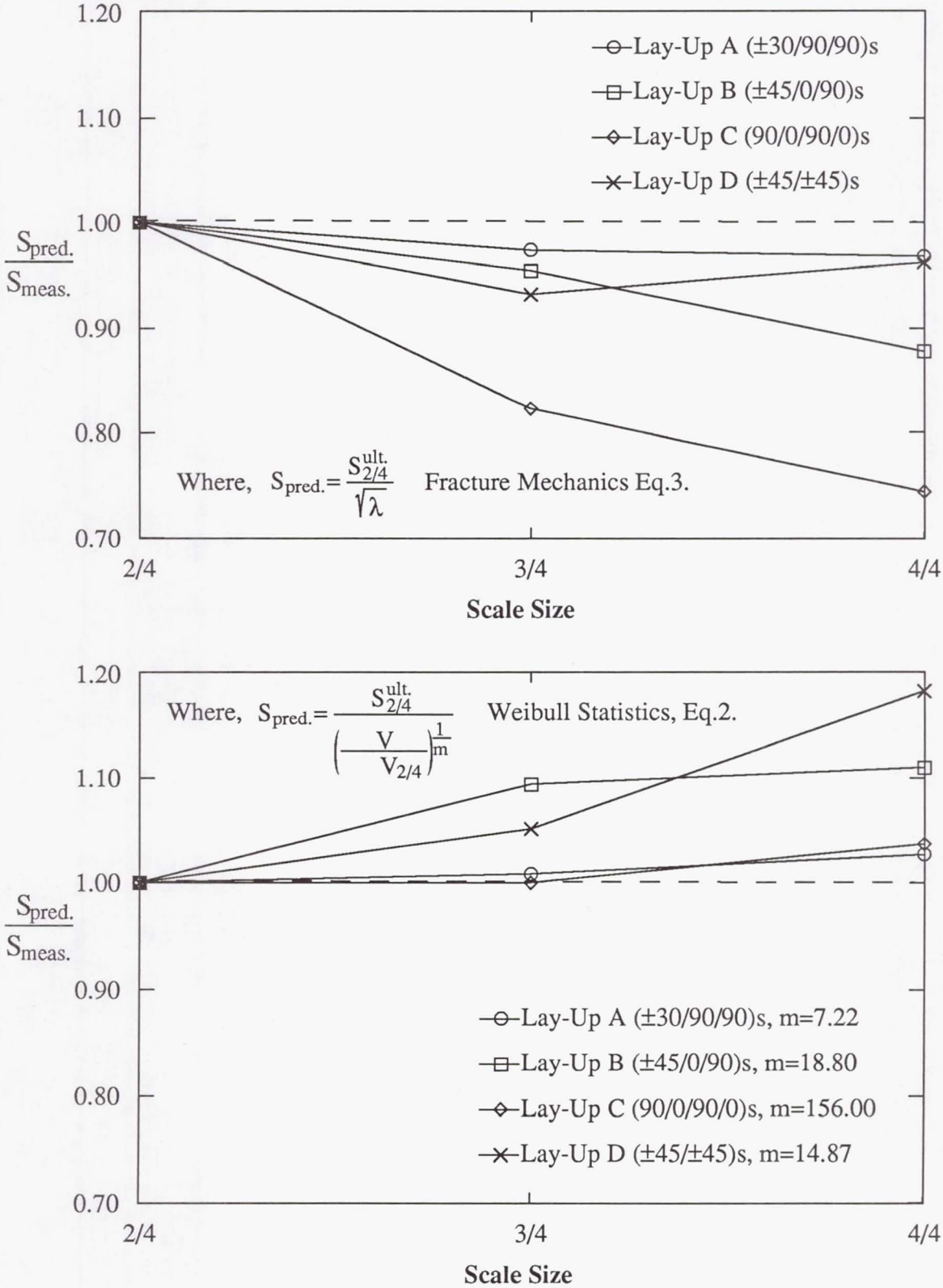

Fig.31 A comparison of the predictive performance between the fracture mechanics based model, Eq.3, and the Weibull statistics based model, Eq.2.

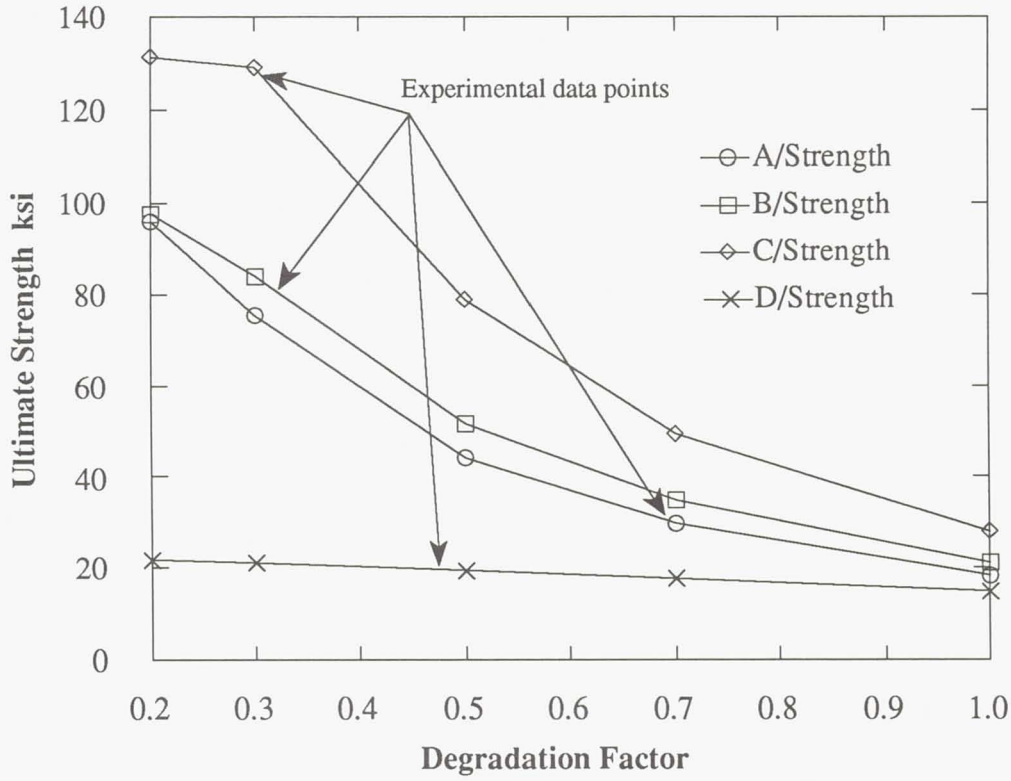

Fig. 32 Calculated strength versus the matrix degradation factor, [9], for lay-ups A, B, C, and D. The strength calculation was based upon the quadratic failure criterion with the strength interaction F*12 assumed to be equal to -0.5.

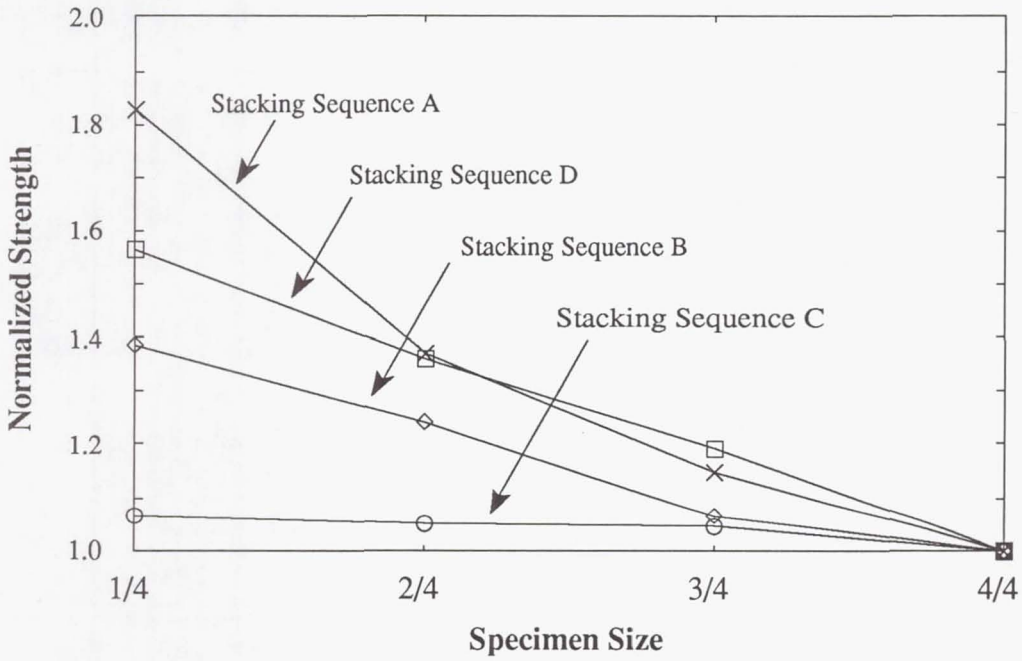

Fig. 33 Normalized strength versus specimen size for lay-ups **A**, **B**, **C**, and **D**. A summary of the experimental results.

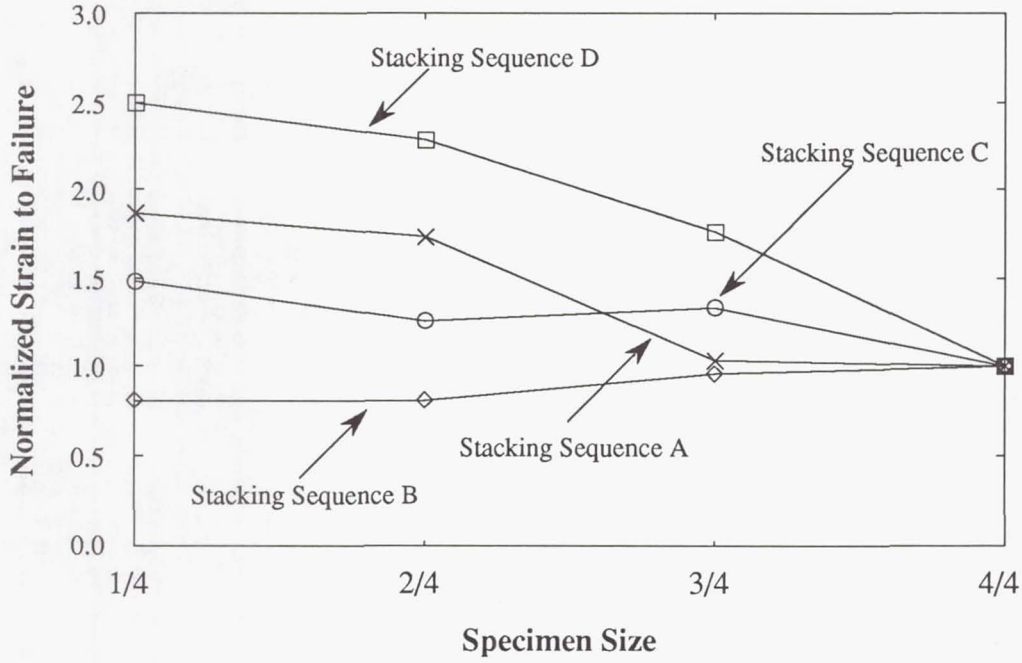

Fig. 34 Normalized strain to failure versus specimen size for lay-ups **A**, **B**, **C**, and **D**. A summary of the experimental results.

NASA
National Aeronautics and Space Administration

Report Documentation Page

1. Report No.	2. Government Accession No.	3. Recipient's Catalog No.
NASA CR-4335		

4. Title and Subtitle	5. Report Date
Strength Scaling in Fiber Composites	November 1990
	6. Performing Organization Code
7. Author(s)	8. Performing Organization Report No.
Sotiris Kellas and John Morton	
	10. Work Unit No.
	505-63-01-11
9. Performing Organization Name and Address	11. Contract or Grant No.
Virginia Polytechnic Institute and State University Dept. of Engineering Science and Mechanics 225 Norris Hall Blacksburg, VA 24061	NAS1-18471
	13. Type of Report and Period Covered
12. Sponsoring Agency Name and Address	Contractor Report
NASA Langley Research Center Hampton, VA 23665-5225	14. Sponsoring Agency Code

15. Supplementary Notes

Langley Technical Monitor: Huey D. Carden

16. Abstract

A research program has been initiated to study and isolate the factors responsible for scale effects in the tensile strength of graphite/epoxy composite laminates. Four lay-ups, $(\pm 30^\circ_n/90^\circ_{2n})_s$, $(\pm 45^\circ_n/0^\circ_n/90^\circ_n/0^\circ_n)_s$, and $(\pm 45^\circ_n/\pm 45^\circ_n)_s$, have been chosen with appropriate stacking sequences so as to highlight individual and interacting failure modes. Four scale sizes have been selected for investigation including full scale size, 3/4, 2/4, and 1/4, with n equal to 4, 3, 2, and 1, respectively. The full scale specimen size was 32 piles thick as compared to 24, 16, and 8 piles for the 3/4, 2/4, and 1/4 specimen sizes respectively. Results were obtained in the form of tensile strength, stress-strain curves and damage development. Problems associated with strength degradation with increasing specimen size have been isolated and discussed. Inconsistencies associated with strain measurements have also been identified. Enhanced X-ray radiography was employed for damage evaluation, following step loading. It has been shown that fiber dominated lay-ups were less sensitive to scaling effects compared to the matrix dominated lay-ups.

17. Key Words (Suggested by Author(s))	18. Distribution Statement
Scaling effects Failure analysis Composite materials Tensile testing	Unclassified - Unlimited Subject category - 39

19. Security Classif. (of this report)	20. Security Classif. (of this page)	21. No. of pages	22. Price
Unclassified	Unclassified	80	A05

NASA FORM 1626 OCT 86

For sale by the National Technical Information Service, Springfield, Virginia 22161-2171

NASA-Langley, 1990